

## **Agenda**

To join, use the ZOOM link or QR code below:

 $\frac{https://us02web.zoom.us/j/86877242631?pwd=WmZiSHRma21CT3ZXOFZPKz}{ZDYWZuQT09}$ 



# The 8th Southeast Asia Collaborative Symposium on Energy Materials (SACSEM 8th) 28-29, Nov. 2022

Invited Speaker: Presentation (15 min.) + Discussion (4 min.) + Change (1 min.) Student Speaker: Presentation (10 min.) + Discussion (4 min.) + Change (1 min.)

### Day 1

### 28th November 2022 (Japan time)

### Chair: Prof. Yohei Yamamoto

Time	No	Affiliation	Presenter	Title	
16:00-16:15	OP	UT	Prof. Yohei Yamamoto	Opening remark and Introduction of research	
				in MI and TREMS	
16:15-16:35	l01	UT	Prof. Takahiro Kondo	Hydrogen boride and boron monosulfide sheets	
16:35-16:55	102	NIMS	Prof. Sepehri Amin	Tunning the hysteresis of magnetic materials by	
			Hossein	microstructure engineering	
16:55-17:15	103	AIST	Prof. Yuichiro Himeda	Development of Catalysts in CO <sub>2</sub> Utilization for	
				Storage and Production of H <sub>2</sub>	
17:15-17:35	104	ITB	Dr. Muhammad Iqbal	In Search of Excellence: Convex versus	
				Concave Noble Metal Nanostructures for	
				Electrocatalytic Applications	
17:35-17:55	105	UKM	Prof. Lorna Jeffery Minggu	Photoelectrochemical Hydrogen Production	
				Using Earth Abundant Metal Oxide	
				Photoelectrodes	
17:55-18:15	106	UKM	Dr. Vidhya Selvanathan	Organosoluble Starch and Cellulose derivatives	
				in DSSC: Unravelling the Synergy between	
				Electrolyte Rheology and Photovoltaic	
				Properties	

18:15-18:30 Short break

### Chair: Assoc. Prof. Takahiro Kondo

Time	No	Affiliation	Presenter	Title
18:30-18:50	107	UTP	Dr. Lila Iznita Izhar	A Preliminary Study on Effectiveness of Brief Mindfulness in Reducing Sress and Anxiety among Students with High Neuroticism based on Peripheral Physiological Data

18:50-19:10	108	KMUTT	Prof. Navadol	Lignin Fractionation and Valorization Platforms
			Laosiripojana	for Converting Potential Biomasses to
				Industrial- Needed Macromolecular Building
				Block Products
19:10-19:30	109	UDE	Dr. Sven Reichenberger	Identification of Structure-Activity Correlations
				by Pulsed Laser Defect Engineering in Liquids
19:30-19:50	l10	UDE	Prof. Heiko Wende	Functional magnetocaloric materials on atomic
				length scales: an element specific perspective
19:50-20:10	l111	ECNU	Prof. Shaoqiang Chen	Lasing Dynamics in Perovskite Microcavities
20:10-20:30	l12	UPD	Prof. Elmer Estacio	Overview of the academic and research
				profiles of the National Institute of Physic,
				University of the Philippines and its work on
				Terahertz optoelectronics
20:30-20:50	l13	KEK	Prof. Kenta Amemiya	Real-time Observation of Surface Chemical
				Reactions by Wavelength-dispersive Soft X-
				ray Absorption Spectroscopy

### Day 2

### 29th November 2021 (Japan time)

### Chair: Prof. Muneaki Hase

Time	No	Affiliation	Presenter	Title
14:00-14:15	S01	UT	Mr. Fadilla Akhmad Fadel	Development of synthesis method for metal- substituted-type $\lambda$ -Ti <sub>3</sub> O <sub>5</sub>
14:15-14:30	S02	UT	Mr. Kentaro Maejima  Abrupt vapor release from porous mol crystal with visible light	
14:30-14:45	S03	ITB	Mr. Fathan Aditya Sanjaya	Study on Mechanism of Fenton Catalyst from Grinding Spark of Waste Metal for Textile Industry Dye Pollutant
14:45-15:00	S04	ITB	Ms. Chandra Wulandari	Modification of Surface Plasmon Resonance (SPR) Biosensor using MoS <sub>2</sub> -MoO <sub>3</sub> Hybrid Microflowers for CFP-10 Tuberculosis Detection
15:00-15:15	S05	ITB	Mr. Muhammad Yovinanda Maulana	Functionalization of Magnetic Fluorescent Silica Nanoparticles with Angiotensin-Converting Enzyme II for Detection of Severe Acute Respiratory Syndrome Coronavirus-2
15:15-15:30	S06	UKM	Ms. Syaza Amira Binti Razali	Deep Eutectic Solvent Assisted Ionothermal Synthesis of Cobalt Based Metal-organic Complex as Electrode Material in Supercapacitors

15:30-15:45	S07	UKM	Mr. Md. Mahfuzul Haque	Developing High Stable Perovskite Solar Cell
				Using RF Magnetron Sputtered Mo-doped
				Tungsten Oxide as Electron Transport Layer
15:45-16:00	S08	UTP	Mr. Mohamad Adil Iman	Molecular Insight into Hybridization of Metal-
			Bin Ishak	Organic Frameworks and Choline-based Ionic
				Liquids (MOF-IL) for Gas Adsorption
16:00-16:15	S09	UTP	Mr. Mohd Sofi Bin Numin	Theoretical Studies of Quaternary Ammonium
				Surfactant Corrosion Inhibitors on Fe (110) in
				Acetic Acid Media via DFT Calculation and MD
				Simulation

16:15-16:30 Short break

### Chair: Assoc. Prof. Masaki Hada

Time	No	Affiliation	Presenter	Title
16:30-16:45	S10	KMUTT	Ms. Chanakarn Piwnuan	Preparation of Au-CsWO <sub>3</sub> Nanocomposites and Near-Infrared Shielding Performance of the Materials: A feasibility study
16:45-17:00	S11	KMUTT	Ms. Wassana Lekkla	Utilization of Cellophane Paper as Flexible Substrates in Perovskite Solar Cells
17:00-17:15	S12	KMUTT	Ms. Saravy Dum	Recovering of Silicon Wafers for Silicon Fine Particles Production
17:15-17:30	S13	UDE	Ms. Johanna Lill	Nuclear resonant scattering for hysteresis design of magnetocaloric materials
17:30-17:45	S14	UDE	Mr. Timo Wagner	Changing surface morphology and chemistry by scalable atmospheric pressure plasma treatment
17:45-18:00	S15	ECNU	Mr. Youyang Wang	Computer-Vision-Aided Solar Cell Defect Detection and Classification in Absolute Electroluminescence Imaging
18:00-18:15	S16	ECNU	Ms. Rui Wang	Improving Vapor-Transport-Deposited Sb <sub>2</sub> S <sub>3</sub> Thin-Film Solar Cells through Source Position Optimization
18:15-18:30	S17	UPD	Mr. Vince Paul Juguilon	Carrier capture dynamics in InAs/GaAs self- assembled quantum dots investigated using time-resolved terahertz spectroscopy
18:30-18:45	S18	UPD	Mr. Jared Operaña	Goos-Hänchen Shifts in low-loss dielectrics: Experimental observations in Si substrate
18:45-	CL	UT	Prof. Muneaki Hase	Closing remark

19:00-	ВА		Discussion Session at Each University

Institut Teknologi Bandung (ITB, Indonesia)

Universiti Kebangsaan Malaysia (UKM, Malaysia)

Universiti Teknologi PETRONAS (UTP, Malaysia)

King Mongkut's University of Technology Thonburi (KMUTT, Thailand)

**Universität Duisburg-Essen (UDE, Germany)** 

East China Normal University (ECNU, China)

University of the Philippines Diliman (UPD, Philippine)

University of Tsukuba (UT, NIMS, AIST, KEK, Japan)



### University of Tsukuba

# UNIVERSITÄT DUISBURG ESSEN



















### **Invited Lectures**

### Hydrogen boride and boron monosulfide sheets

### Takahiro Kondo<sup>1</sup>

<sup>1</sup>Faculty of Pure and Applied Sciences, University of Tsukuba, Japan E-mail: takahiro@ims.tsukuba.ac.jp

As new 2D metal-free materials, we have reported boron monosulfide (BS) sheets [1] and hydrogen boride (HB) sheets [2]. The BS sheets are crystalline semiconductor and its bandgap was found to be tuned to a desired value by



controlling the number of stacked 2D BS nanosheet [1]. HB sheets are composed of boron and hydrogen at a 1:1 stoichiometric ratio, which can be formed by an ion-exchange reaction between protons and magnesium cations in magnesium diboride with exfoliation [2]. In the HB sheets, boron atoms form a hexagonal 2D network, in which hydrogen atoms are bound to boron by three-center-two-electron bonds (B–H–B) and two-center-two-electron bonds (B–H) [3]. Experimental studies have clarified that HB sheets exhibit solid acid catalytic activity [4], metal ion reducibility [5, 6], semimetal electronic properties [7], gas-sensor applicability [3], stability against water [8], CO<sub>2</sub> adsorption/conversion property including C-C coupling [9], and a light-responsive hydrogen release function [10]. Furthermore, theoretical studies have revealed intriguing electronic [11] optical, and thermal properties [12], as well as possible applications of HB sheets as rechargeable Li/Na ion battery electrodes [13], hydrogen release [14], reversible hydrogen storage [15], current limiting [16], photodetectors, individual identification of amino acids [17], and anodes for rechargeable potassium-ion batteries with a high capacity, low voltage, and desirable rate performance. In this talk, the synthesis, evaluation, and application of HB and BS sheets will be presented.

### Acknowledgement

These works were done with Mr. H. Nishino, Prof. T. Fujita, Dr. N. T. Cuong, Dr. S. Tominaka, Prof. M. Miyauchi, Dr. S. Iimura, Dr. A. Hirata, Dr. N. Umezawa, Prof. S. Okada, Prof. E. Nishibori, Mr. A. Fujino, Mr. R. Ishibiki, Mr. T. Goto, Mr. H. Kusaka, Dr. M. Toyoda, Prof. T. Tokunaga, Prof. A. Yamamoto, Dr. M. Miyakawa, Dr. K. Horiba, Prof. S. Saito, Dr. T. Taniguchi, Dr. K. Watanabe, Dr. S. Shinde, Ms. L. Li, Prof. T. Sakurai, Ms. M. Lima, Mr. K. Miyazaki, Mr. K. Matsushita, Dr. M. Masuda, Proi. I. Hamada, Prof. Y. Morikawa, Dr. A. Yamaguchi, Mr. R. Kawamura, Dr. S. Ito, Dr. Tateishi, Prof. Niibe, Prof. J. N. Kondo, Dr. T. Fujitani, Prof. I. Matsuda, Prof. J. Nakamura, and Prof. H. Hosono.

#### References

- [1] H. Kusaka, R. Ishibiki, M. Toyoda, et al., J. Mater. Chem. A, 9, 24631 (2021).
- [2] H. Nishino, T. Fujita, N. T. Cuong, S. Tominaka, et al., J. Am. Chem. Soc. 139, 13761 (2017).
- [3] S. Tominaka, R. Ishibiki, A. Fujino, K. Kawakami, et al., Chem, 6, 406 (2020).
- [4] A. Fujino, et al., ACS Omega, 4, 14100 (2019). A. Fujino, et al., PCCP 23, 7724 (2021).
- [5] S. I. Ito, T. Hirabayashi, R. Ishibiki, R. Kawamura, et al., Chem. Lett. 49, 789 (2020).
- [6] S. Gao, Y. Zhang, J. Bi, B. Wang, C. Li, J. Liu, et al., J. Mater. Chem. A, 8, 18856 (2020).
- [7] I. Tateishi, N. T. Cuong, C. A. S. Moura, et al. Phys. Rev. Mate. 3, 024004 (2019).
- [8] K. I. Rojas, N. T. Cuong, H. Nishino, Commun. Mate. 2, 81 (2021).
- [9] T. Goto, S. Ito, S. L. Shindem et al., Commun. Chem. 5, 118 (2022).
- [10] R. Kawamura, N. Cuong, T. Fujita, R. Ishibiki, et al., Nat. Commun., 10, 4880 (2019).
- [11] Y. Jiao, F. Ma, J. Bell, A. Bilic, A. Du, Angew. Chemie Int. Ed. 55, 10292 (2016).
- [12] B. Mortazavi, et al, Nanoscale, 10, 3759 (2018); J. He, et al, NPJ Comput. Mater. 5, 47 (2019).
- [13] V. Shukla, et al., PCCP. 20, 22008 (2018); M. Makaremi, et al., Mater. Today Energy 8, 22 (2018).
- [14] T. A. Abtew, et al., Phys. Rev. B, 83, 094108 (2011); Phys. Rev. B, 84, 094303 (2011).
- [15] L. Chen, X. Chen, C. Duan, Y. Huang, et al., Phys. Chem. Chem. Phys. 20, 30304 (2018).
- [16] Y. An, Y. Hou, H. Wang, J. Li, R. Wu, et al., Phys. Rev. Appl. 11, 064031 (2019).
- [17] P. Xiang, X. Chen, B. Xiao, Z. M. Wang, ACS Appl. Mater. Interfaces, 11, 8115 (2019).

# Tunning the hysteresis of magnetic materials by microstructure engineering

<u>H. Sepehri-Amin<sup>1,2</sup>,</u> Xin Tang<sup>1</sup>, J. S. Zhang<sup>1</sup>, E. Dengina<sup>1,2</sup>, A. Bolyachkin<sup>1</sup>, T. Ohkubo<sup>1</sup>, K. Hono<sup>1,2</sup>

<sup>1</sup>National Institute for Materials Science, Tsukuba, Japan

<sup>2</sup>Faculty of Pure and Applied Sciences, University of Tsukuba, Tsukuba, Japan

E-mail: h.sepehriamin@nims.go.jp



Magnetic materials are essential component for the green energy conversion and data storage and they play critical role toward realization of carbon neutral society. One of the key factors that can result in different functionality in the magnetic materials is so called "hysteresis". Hysteresis can be controlled through several intrinsic and extrinsic parameters. Design of materials and their microstructure in a broad length scale from atomic, to nano and micro-scale can influence the magnet's hysteresis and their functionality. In this talk, we will discuss the hysteresis requirement for different applications of the magnetic materials; *i. e.* realizing a large magnetic hysteresis is desired for permanent magnets and magnetic recording media while reduction of hysteresis is needed for soft magnets and magnetocaloric materials.

In the first part of presentation, we will show our recent success in realizing a sufficiently large coercivity of 1.0 T in rare-earth lean SmFe<sub>12</sub>-based anisotropic magnets assisted by machine learning (Fig. 1) [1-4]. Based on detailed microstructure characterizations and micromagnetic simulations, we will discuss the optimum microstructure which can lead to a larger coercivity and remanent magnetization in the anisotropic bulk sintered SmFe<sub>12</sub>-based magnets which have potential to realize the next generation high performance permanent magnets. In the second part of my talk, we will present our research activity on development of hysteresis free magnetocaloric materials with a large magnetocaloric effect for the efficient and environmental benign cryogenic magnetic refrigeration applications [5-7].

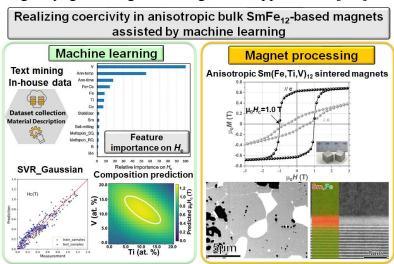


Fig. 1. Development of anisotropic SmFe<sub>12</sub>-based sintered magnet with sufficiently large coercivity of 1.0 T assisted by machine learning [1-4].

- [1] H. Sepehri-Amin et al. Acta Mater. 194 (2020) 337. [2] X. Tang et al. Scripta Mater. 200 (2021) 113925.
- [3] J. S. Zhang et al. Acta Mater. 217 (2021) 117161. [4] J. S. Zhang et al. Acta Mater. 238 (2022) 118228.
- [5] J. Lai, et al. Acta Mater. 232 (2022) 117942. [6] J. Lai, H. Sepehri-Amin, et al. Acta Mater. 220 (2021) 117286
- [7] Xin Tang, H. Sepehri-Amin, et al. Nature Communications 13 (2022) 1.

# Development of Catalysts in CO<sub>2</sub> Utilization for Storage and Production of H<sub>2</sub>

Yuichiro Himeda<sup>1,2</sup>

<sup>1</sup>National Institute of Advanced Industrial Science and Technology (AIST), 16-1 Onogawa, Tsukuba, Ibaraki 305-8569, Japan

<sup>2</sup>Faculty of Pure and Applied Sciences, University of Tsukuba, Tsukuba, Japan E-mail: himeda.y@aist.go.jp



Conversion of thermodynamically stable CO<sub>2</sub> requires highly efficient catalyst. Herein, we describe highly effective catalysts for CO<sub>2</sub> hydrogenation to formate and methanol, and dehydrogenation of formic acid. <sup>[1]</sup>

### (1) Catalyst development for CO<sub>2</sub> hydrogenation to formate in water <sup>[2]</sup>

Half-sandwich iridium complexes with N,N'-bidentate ligand serve as a catalyst for CO<sub>2</sub> hydrogenation to formate in water. We have revealed that (i) enhancement of catalytic activity by strong electro-donating effect from oxyanion formed by deprotonation of hydroxyl group, and (ii) acceleration of hydride complex formation by second coordination sphere interaction such as pendent base effects.<sup>[2d]</sup>

### (2) High-pressure H<sub>2</sub> production by dehydrogenation of formic acid <sup>[3]</sup>

Formic acid (FA) is known as liquid organic hydrogen carrier (4.4wt% of H<sub>2</sub>). We have developed highly efficient and durable iridium catalysts in acidic aqueous solution. Interestingly, FA dehydrogenation in water can supply high-pressure gases (up to 157 MPa) in closed vessel. Furthermore, high-pressure H<sub>2</sub> gas separation from the generated gas simply by cooling the gas were demonstrated.

### (3) Methanol production by CO<sub>2</sub> hydrogenation using dinuclear catalyst **2** in gas-solid phase reaction <sup>[4]</sup>

Novel approach toward the catalytic hydrogenation of CO<sub>2</sub> to methanol in the gas-solid phase using dinuclear iridium complexes **2** at near room temperature are described. [4a] CO<sub>2</sub> hydrogenation in water catalyzed by mononuclear iridium catalyst **1** provided mainly FA but a negligible amount of methanol. On the other hand, the combination of a dinuclear catalyst **2** and gas-solid phase reaction conditions led to the effective production of methanol from CO<sub>2</sub>. Conveniently, methanol obtained from the gas phase could be easily isolated from the catalyst without contamination with CO, CH<sub>4</sub>, or FA. The high catalytic activity has been attributed to hydride complex formation upon exposure to H<sub>2</sub> gas, suppression of the liberation of FA under gas-solid phase reaction conditions, and intramolecular multiple hydride transfer to CO<sub>2</sub> by the multinuclear catalyst.

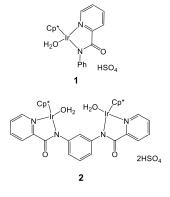


Fig. 3. Catalysts for CO<sub>2</sub> hydrogenation

### References

[1] a) Chem. Rev. **2015**, 115, 12936. b) Coord. Chem. Rev. **2018**, 373, 317. c) Advanced Energy Materials **2019**, 9, 1801275. d) CO<sub>2</sub> Hydrogenation Catalysis, Wiley, 2021.

[2] a) Organometallics **2004**, 23, 1480; b) Organometallics **2007**, 26, 702–712. c) ACS Catal. **2013**, 3, 856; d) Nat. Chem. **2012**, 4, 383; e) Organometallics **2020**, 39, 1519.

[3] a) Green Chem. **2009**, 11, 2018; b) Adv. Synth. Catal. **2019**, 361, 289; c) ChemCatChem **2016**, 8, 886; d) Inorg. Chem. **2020**, 59, 4191.

[4] a) J. Am. Chem. Soc. 2021, 143, 1570; b) Chem Catal. 2022, 2, 242. c) Coord. Chem. Rev. 2022, 472, 214767.

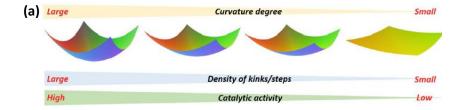
# In Search of Excellence: Convex versus Concave Noble Metal Nanostructures for Electrocatalytic Applications

Muhammad Iqbal<sup>1,2,3</sup>, Yoshio Bando<sup>3,4</sup>, Ziqi Sun<sup>5</sup>, Kevin C.-W. Wu<sup>6</sup>, Alan E. Rowan<sup>7</sup>, Jongbeom Na<sup>7</sup>, Bu Yuan Guan<sup>8,9</sup>, Yusuke Yamauchi<sup>1,7</sup>

<sup>1</sup>JST-ERATO Yamauchi Materials Space-Tectonics Project, International Center for Materials Nanoarchitectonics (WPI-MANA), National Institute for Materials Science (NIMS), 1-1 Namiki, Tsukuba, Ibaraki, 305-0044 Japan <sup>2</sup>Advanced Functional Materials Research Group, Institute of Technology Bandung, Ganesha 10, Indonesia 40132 <sup>3</sup>Institute of Molecular Plus, Tianjin University, No. 11 Building, No. 92 Weijin Road, Nankai District, Tianjin, 300072 P. R. China <sup>4</sup>Australian Institute of Innovative Materials, University of Wollongong, Squires Way, North Wollongong, New South Wales, 2500 Australia <sup>5</sup>School of Chemistry and Physics, Queensland University of Technology, Brisbane, Queensland, 4000 Australia <sup>6</sup>Department of Chemical Engineering, National Taiwan University, Taipei, 10617 Taiwan <sup>7</sup>Australian Institute for Bioengineering and Nanotechnology (AIBN), The University of Queensland, Brisbane, Queensland, 4072 Australia <sup>8</sup>State Key Laboratory of Inorganic Synthesis and Preparative Chemistry, College of Chemistry, Jilin University, Changchun, 130012 P. R. China <sup>9</sup>Joint Research Center for Future Materials, International Center of Future Science, Jilin University, Qianjin Street 2699, Changchun, 130012 P. R. China

E-mail: muh.iqbal@itb.ac.id

Controlling the shape of noble metal nanoparticles is a challenging but important task in electrocatalysis. Apart from hollow and nanocage structures, concave noble metal nanoparticles are considered a new class of unconventional electrocatalysts that exhibit superior electrocatalytic properties as compared with those of conventional nanoparticles (including convex and flat ones). Several facile and highly reproducible routes for synthesizing nanostructured concave noble metal materials has been reported in the literature, together with their advantages over noble metal nanoparticles with convex shapes. The routes are including seed-mediated synthesis, facet-selective etching synthesis, facet-selective binding synthesis, and micelle-assisted synthesis [1]. Nanostructured noble metals with concave features are found to show better catalytic activity and stability hence improve their practical applicability in electrocatalysis. The presense of surface defects and structural stability are found to be responsible for the improvement of catalytis activity and stability of concave noble metal nanocatalyst (Fig. 1a). We shows an example of concave mesooporous Pd nanocrystals (MPNs) which fabricated through micelle-assisted synthesis and shows enhanced electrocatalytic activity than that of conventional spherical nanocrystals (Fig. 1b) [2].



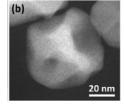


Fig. 1 (a) Relationship among the curvature degrees of concave nanocrystals, density of kinks/steps, and expected catalytic activity and (b) HAADF-STEM image of one typical concave mesoporous Pd nanocrystals.

### References

[1] M. Iqbal et al., Adv. Mat. 2021, 33, 2004554. [2] M. Iqbal et al., ACS Appl. Mater. Interfaces, 2020, 12, 51357-51365.

### 8th SACSEM Symposium

#### **Abstract**



# Photoelectrochemical Hydrogen Production Using Earth Abundant Metal Oxide Photoelectrodes

Nur Azlina Adris<sup>1</sup>, Noradiba Nordin<sup>1</sup>, Lorna Jeffery Minggu<sup>1</sup>\*

<sup>1</sup>Fuel Cell Institute, Universiti Kebangsaan Malaysia, 43600 UKM Bangi, Selangor Darul Ehsan, Malaysia \*Corresponding author: lorna\_jm@ukm.edu.my

Direct hydrogen production from water splitting by sunlight is very attractive to address the world renewable and sustainable energy needs. Water is plentiful and the product after using hydrogen as fuel is also water hence, the cycle of generation and consumption forms a continuous loop. Photoelectrochemical (PEC) water splitting is a very promising green method to produce hydrogen. The main component in PEC is the photoactive material which has to fulfil the requirements of suitable bandgap and band edges and also high stability in water and relatively low cost. Due to the abundance of copper, as well as its favourable band gap and alignment, cuprous oxide (Cu<sub>2</sub>O) based photocathodes is a potential material for PEC water splitting. Besides, hematite (Fe<sub>2</sub>O<sub>3</sub>) also is a low-cost material with good chemical stability in an aqueous solution. The performance of Cu<sub>2</sub>O and Fe<sub>2</sub>O<sub>3</sub> based photoelectrodes prepared by facile electrodeposition method towards PEC water splitting is presented. The Cu<sub>2</sub>O electrodeposited on FTO with intermediate layer shows improvement in photocurrent as photocathode. While Fe<sub>2</sub>O<sub>3</sub> deposited on nickel foam shows significant photocurrent as photoanode.

# Organosoluble Starch and Cellulose derivatives in DSSC: Unravelling the Synergy between Electrolyte Rheology and Photovoltaic Properties

Vidhya Selvanathan

- <sup>a</sup> Solar Energy Research Institute (SERI), Universiti Kebangsaan Malaysia(UKM), 43600 Bangi, Selangor, Malaysia
- b Department of Electrical, Electronic and Systems Engineering, Faculty of Engineering and Built Environment, Universiti Kebangsaan Malaysia, 43600 Bangi, Selangor, Malaysia.



E-mail: vidhya@ukm.edu.my

In this work, a simple phthaloylation process involving reaction of starch with phthalic anhydride is proposed to transform starch into organosoluble material. FTIR and NMR spectroscopy results verifies the formation of phthaloyl starch (PhSt). The resulting starch derivative, was then blend with hydroxyethyl cellulose (HEC) to fabricate polymer gel electrolytes. Rheological analyses such as amplitude sweep studies and tack tests indicate that gels with good rigidity, strength and adhesiveness were attained upon blending 20 to 60 wt.% HEC. Gels within this optimum range of composition were then fabricated into quasi-solid dye-sensitized solar cell (QSDSSC) with the addition of 5 wt.% of tetrapropylammonium iodide and iodine. EIS of the QSDSSC reveal that the adhesive property of the gels plays a crucial role in affecting charge transfer processes at the electrode/electrolyte interfaces. The highest efficiency of 3.02% was recorded with the gels consisting 70 wt.% of PhSt and 30 wt.% of HEC. This polymer blend composition was then used to study the effect of salt composition on the electrolyte properties in which two series of polymer gels containing different amounts of tetrapropylammonium iodide (TPAI) and lithium iodide (LiI) respectively were prepared. Storage modulus values from rheological studies showed that the size of cations in the electrolytes affects the mechanical property of the gels. Best performing solar cells with the efficiency of 3.94 % was achieved by addition of 12.5 wt.% of TPAI. As an initiative to further boost the efficiency values, 1-butyl-3-methylimidazolium iodide (BMII) was included into the PhSt-HEC-TPAI system. The ionic liquid greatly enhanced the short circuit current of the cells, leading to an optimum efficiency of 5.20 % upon addition of 8 wt.% of BMII.

# A Preliminary Study on Effectiveness of Brief Mindfulness in Reducing Sress and Anxiety among Students with High Neuroticism based on Peripheral Physiological Data



Nik Amalia Nadirah Nik Rashidi<sup>1</sup>, Ir Dr Patrick Sebastian<sup>1</sup>, AP Ir Dr Irraivan Elamvazuthi<sup>1</sup>, Dr Lila Iznita Izhar<sup>1</sup>

<sup>1</sup> Smart Assistive and Rehabilitative Technology Research Group, Institute of Health and Analytics, Electrical and Electronic Engineering Department, Universiti Teknologi PETRONAS Perak, Malaysia

E-mail: <u>nik\_20001944@utp.edu.my</u>

Due to the circumstances from internal as well as external such as relationship problem, low self-confidence and academic pressure, stress can be a major problem among university students. In this research, the focus area is to assess stress among university students based on subjective and objective measurement tools. Self-report questionnaires were administered to gain subjective measurement while EEG and peripheral biosignals such as Blood Volume Pulse (BVP), Skin Conductance (SC) and Respiratory Rate (RR) were also acquired as the objective based measurement and analysis on effectiveness of brief mindfulness-based intervention (MI) in improving relaxation and thus potentially reducing stress. Both measurement tools can help to assess on the effect of brief mindfulness among the subjects in coping with stress-induced activity (watching of emotional video clips) and performing Stroop Task. Some of the instruments administered for the subjective assessments are namely the Depression, Anxiety and Stress Scale (DASS) 21 and The National Aeronautics and Space Administration Task Load Index (NASA-TLX). These subjective measurements were rated by the subjects during pre-MI and post-MI to assess the severity of symptoms associated with depression, anxiety and stress, and to measure workload after completing a task respectively.

Paired t-test analysis was performed in this study to evaluate changes in the results from the questionnaires and peripheral biosignals between pre- and post-MI. Based on the DASS-21 and NASA-TLX analysis, few parameters were shown to give significant changes (p<0.05) such as anxiety and stress parameter in DASS-21, and mental, physical, and temporal demand dimensions, as well as effort in NASA-TLX. Furthermore, significant decrease in the scores for anxiety (p=0.0017) and stress (p=0.0057) between pre- and post-MI was obtained. These results may indicate the improvement on stress and anxiety management achieved through MI. In objective measurement analysis, it was found that the SC showed the most significant change with p=0.0016 compared to that of BVP (p=0.4824) and RR (p=0.2286) during Stroop Task based cognitive assessment, during the resting states and Stroop Task. Hence, SC can be a potential indicator for the effectiveness of MI in helping students to cope with stress better and to improve their relaxation level. Future studies should investigate further the SC as a potential parameter in identifying effectiveness of mindfulness for better management of stress and improvement in relaxation and to use larger sample to provide more accurate findings and correlations.

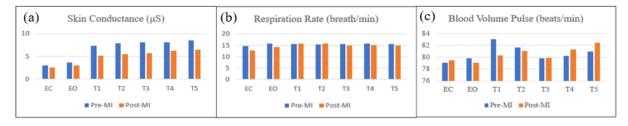


Fig. 1. Performance during baseline (eyes-closed (EC), eyes-opened (EO)), and trials (T1-T5) based on (a) SC (b) RR and (c) BVP averaged values for 15 subjects.

### Lignin Fractionation and Valorization Platforms for Converting Potential Biomasses to Industrial-Needed Macromolecular Building Block Products

Navadol Laosiripojana

The Joint Graduate School of Energy and Environment, King Mongkut's University of Technology Thonburi (KMUTT), Bangkok, Thailand



E-mail: navadol.lao@kmutt.ac.th

Conversion of lignocellulosic agricultural biomass to biofuels, biochemical, and biomaterials is a promising sustainable alternative platform industry to the current petroleum-based industry with the advantages on renewable and carbon-neutral nature of the starting materials. This socalled "biorefinery" industry has received great attention as a new economic driver in bioeconomy worldwide. Lignocellulose is a complex structure comprising cellulose microfibers connected to hemicellulose matrix which formed networks to the lignin shield, making plant cell wall recalcitrant to chemical or biological decomposition. Fractionation of lignocellulose components is an initial pre-requisite step in integrated biorefineries where the individual separated biopolymers are processed to a spectrum of products using multi-discipinary technology with a near-zero waste concept. Clean fractionation (CF) is one of the pretreatment processes to separate the cellulose, hemicellulose, and lignin from the biomass. In this process, organic solvents such as alcohols, ketones, esters, and organic acids and/or mixed with water are used without the presence of catalyst. Lignin obtained by this process and other pretreatments are modified and have an increased proportion of condensed C-C linkages and reduced amount of β-O-4 bonds both of which negatively impact on the depolymerization process. The challenge for lignin valorization is to develop operating processing conditions so that a narrow range of targeted products can be obtained. It is well known that zeolite-based catalysts have been extensively used in refineries and petrochemical industries for cracking, dehydrogenation, dealkylation, and isomerisation reactions as a result of their excellent catalytic performance and low cost. Besides the composition and structure of the zeolite catalyst, the solvent type has been shown to increase lignin depolymerisation, reduce char formation and reduce repolymerisation reactions. Methyl isobutyl ketone (MIBK) is one of the solvent that has only received limited investigation. The role it plays (as well as other solvents) in the formation phenolic monomers from lignin velarization is not well understood. Another approach to develop commercial viable technologies based on technical lignins (such as organosolv lignin) is to target the production of groups of similar chemical classes rather than individual compounds, reducing costly separation and purification costs. In most lignin depolymerization reactions, oligomeric and polymeric lignin species still persist, even under mild conditions. The evidence from previous studies showed that lignin during depolymerization, because of its nature, form reactive species e.g., quinone compounds, and so it is energetically favourable for it to repolymerize to form oligomers and polymers. This problem statement opened up a new research approach towards sustainable catalytic conversion of lignin into functional compounds, which hitherto has not been exploited for a one-pot cleave and couple synthesis.

### Identification of Structure-Activity Correlations by Pulsed Laser Defect Engineering in Liquids

S. Zerebecki1, S. Barcikowski1,

### S. Reichenberger1

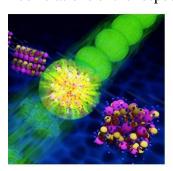
<sup>1</sup>Technical Chemistry I and Center for Nanointegration Duisburg-Essen (CENIDE), Research Center for Nano Energy Technology (NETZ), Duisburg, 47057, University of Duisburg-Essen, Germany

E-mail: <a href="mailto:sven.reichenberger@uni-due.de">sven.reichenberger@uni-due.de</a>



Point, line, planar, and bulk crystallographic defects are common in solid oxide materials and contribute significantly to their catalytic activity and selectivity. Yet, identifying correlations between their catalytic activity and the amount of material defects demands a catalyst synthesis and/or post-processing that allows to independently alter the defect density of the catalyst while maintaining the other activity-relevant properties like particle size, BET surface area, composition, or crystal phase. Due to the intrinsic flexibility of the cation occupancy spinel ferrites and cobaltites represent a particularly interesting material class to investigate such defect- related activity trends in oxidation catalysis.

This talk intends to summarize our current breakthroughs in laser-based writing gradual defect densities into spinel cobaltites and ferrites to identify related structure-activity correlations in heterogeneous catalysis. Hereby, a flat liquid jet setup was used to gradually laser-post-process Co O <sup>[1]</sup> and CoFe O <sup>[2]</sup> with single laser pulses and tune the occupancy of octa- and tetrahedral sites. Additionally, the laser-based diffusion enhancement to achieve a catalyst surface doping<sup>[3]</sup> will be presented. The observed effects of structural disordering including the occupancy of cations in octahedral and tetrahedral sites will be discussed. Based on the developed gradually defect-engineered spinels their catalytic activity in electro- and oxidation catalysis will be discussed providing an outlook on the underlying structure-activity correlations of the respective spinel-based catalysts.



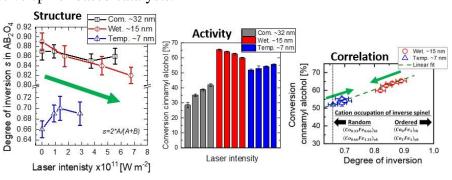


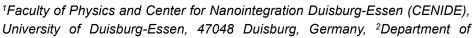
Figure 1: Artwork on pulsed laser defect engineering in liquid (PUDEL) with single laser pulses and uniform laser intensity (right) and a related study of a structure-activity-correlation in oxidation catalysis using a gradually laser-modified catalyst series (here CoFe<sub>2</sub>O<sub>4</sub>).[1]

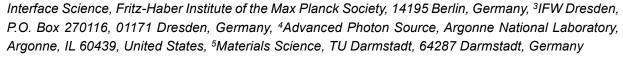
### References

- [1] E. Budiyanto, S. Zerebecki, C. Weidenthaler, T. Kox, S. Kenmoe, E. Spohr, S. DeBeer, O. Rüdiger, S. Reichenberger, S. Barcikowski, and H. Tüysüz, *ACS Appl. Mater. Interfaces*, 13, 44, 2021
- [2] S. Zerebecki, S. Salamon, J. Landers, Y. Yang, Y. Tong, E. Budiyanto, D. Waffel, M. Dreyer, S. Saddeler, T. Kox, S. Kenmoe, E. Spohr, S. Schulz, M. Behrens, M. Muhler, H. Tüysüz, R. K. Campen, H. Wende, et al., ChemCatChem, 2022, 10.1002/cctc.202101785
- [3] S. Zerebecki, K. Schott, S. Salamon, J. Landers, H. Wende, E. Budiyanto, H. Tüysüz, S. Barcikowski, and S. Reichenberger, *J. Phys. Chem. C*, vol. 126, no. 36, pp. 15144–15155, 2022

# Functional magnetocaloric materials on atomic length scales: an element specific perspective

M. E. Gruner<sup>1</sup>, B. Eggert<sup>1</sup>, J. Lill<sup>1</sup>, J. Landers<sup>1</sup>, S. Salamon<sup>1</sup>, A. Terwey<sup>1</sup>, W. Keune<sup>1</sup>, B. Roldán Cuenya<sup>2</sup>, C. Weis<sup>1</sup>, S. Makarov<sup>1</sup>, D. Klar<sup>1</sup>, M. Krautz<sup>3</sup>, J. Zhao<sup>4</sup>, M. Y. Hu<sup>4</sup>, T. S. Toellner<sup>4</sup>, E. E. Alp<sup>4</sup>, K. Ollefs<sup>1</sup>, O. Gutfleisch<sup>5</sup>, <u>H. Wende<sup>1</sup></u>





E-mail: heiko.wende@uni-due.de

Bulk magnetic materials enable an efficient energy conversion and therefore play a crucial role for sustainable energy-related technologies. While new permanent magnets are essential for wind turbines, e-mobility and robotics, bulk magnetocaloric materials open new routes for solid statebased refrigeration. In contrast to permanent magnets with a maximized magnetic hysteresis, magnetocaloric systems shall present a minimized (thermal) hysteresis [1,2] (see Fig. 1). The tailoring of hysteresis in the magnetocaloric systems is a crucial task which is tackled by modifying structural phase transitions. To understand the interplay of local atomic magnetic properties with the lattice dynamics, the study of element specific thermodynamics is essential for the analysis of the coupling of lattice and magnetic degrees of freedom [3,4]. I will demonstrate how element specific techniques can be employed to achieve a fundamental understanding of the hysteresis on atomic length scales. Examples will be presented for the magnetocaloric materials LaFe<sub>13-x</sub>Si<sub>x</sub> [3-6] and FeRh [7,8]. The comparison of the experimental observations to results by density functional theory enables the disclosure of the cross-coupling between magnetic, electronic and vibrational degrees of freedom. This will allow us to develop design rules for magnetocaloric materials that are specifically tailored for innovative applications across all relevant length scales.

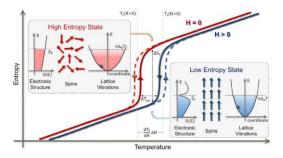


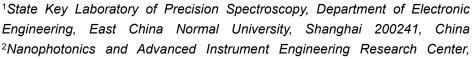
Fig. 1. Schematic T–S diagram illustrating the magnetocaloric effect at a first-order transition. Application of a magnetic field H shifts the transformation temperature  $T_t$  to higher values. Applying the magnetic field isothermally in the intermediate temperature range between  $T_t$  (H=0) and  $T_t$  (H>0) leads to a decrease of  $\Delta S_T$  in the total entropy, whereas an adiabatic field release decreases the temperature by  $\Delta T_{ac}$ , which can be used for heat transport or cooling (figure taken from Ref. [1]).

#### References

[1] F. Scheibel et al., Energy Technol. **6 (8)**, 1397-1428 (2018). [2] O. Gutfleisch et al., Phil. Trans. R. Soc. A **347**, 20150308 (2016). [3] M. E. Gruner et al., Phys. Rev. Lett. **114**, 057202 (2015). [4] M. E. Gruner et al., Phys. Status Solidi B **255**, 1700465 (2018). [5] A. Terwey et al., Phys. Rev. B **101**, 064415 (2020). [6] J. Landers et al., Phys. Rev. B **98**, 024417 (2018). [7] B. Eggert et al., RSC Adv. **10**, 14386-14395 (2020). [8] M. Wolloch et al., Phys. Rev. B **94**, 174435 (2016).

### **Lasing Dynamics in Perovskite Microcavities**

<u>Shaoqiang Chen</u><sup>1,2</sup>, Guoen Weng<sup>1</sup>, Xiaobo Hu<sup>1</sup>, Chunhu Zhao<sup>1</sup>, Jiao Tian<sup>1</sup>, Jiyu Yan<sup>1</sup>, Hanbing Zhang<sup>1</sup>, Shengjie Chen<sup>1</sup>, Jialong Bao<sup>1</sup>, Junhao Chu<sup>2</sup>, Hidefumi Akiyama<sup>3</sup>





Ministry of Education, East China Normal University, Shanghai 200241, China. <sup>3</sup>Institute for Solid State Physics, The University of Tokyo, Kashiwanoha 5-1-5, Kashiwa, Chiba 2778581, Japan

E-mail: sqchen@ee.ecnu.edu.cn

Perovskite materials with excellent optoelectronic properties, have shown remarkable progresses in the field of not only solar cells but also light emitting devices, such as perovskite-based vertical cavity surface emitting lasers (VCSEL) and distributed feedback (DFB) lasers, and very fascinating single-mode lasing properties have been demonstrated [1].

To study the detailed lasing mechanisms in perovskite based microcavities, we have fabricated various kinds of CsPbBr3 perovskite micro-cavities, such as micro-hemispheres, microplates, micro-rods, and micro-cubes, on different substrates, with a size from several tens to 200 micrometers. All the microcavities show lasing behaviors under femtosecond optical excitations, with Fabry-Perot mode and/or whispering-gallery mode. The higher carrier density more that Mott density at lasing threshold indicates the lasing behavior in these perovskite microcavities should mainly be related to electron-hole plasma rather than exciton [2].

The spectrally- and temporally-resolved lasing images of the microcavities with a streak camera, show two importance lasing features of the microcavities with increasing excitation fluences, one is the redshift of the dominant lasing spectra to low energy side due to the band gap renormalization (BGR) effect, another one is the blueshift of each lasing mode to higher energy side due to the reduction of the refractive index caused by the high injection carrier density. The lasing dynamics is merged with the transient BGR effect and the transient change of refractive index in perovskite microcavities [3].

We also fabricated CsPbBr3 perovskite nanocrystals based VCSEL, and single-mode lasing has been observed. With an excitation power over 2 times of the threshold, short pulses with a pulse width around 23 ps have been obtained, the lasing dynamics has been demonstrated to be gain-switching related, indicating a potential application in short pulse generation of perovskite based VCSELs [4].

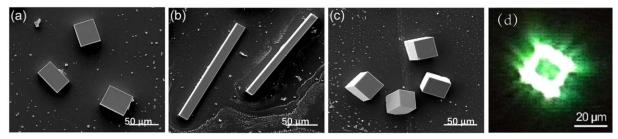


Fig. 1. Several kinds of CsPbBr3 perovskite micro-cavities on silicon(a), sapphire(b) and quartz(c) substrates, and lasing imaging under microscopy of the cubic microcavities excited with femtosecond laser beam.

### References

[1]C. Zhao et al., Chemical Engineering Journal.**2021**.*420*,127660. [2]G. Weng et al., ACS Photonics.**2021**.*8*, 787-797. [3]G. Weng et al., Photonics Research. **2021**. *9*, 54. [4]J. Tian et al., Communications Physics. **2022**.*5*,160.

### Overview of the academic and research profiles of the National Institute of Physic, University of the Philippines and its work on Terahertz optoelectronics



Elmer S. Estacio

National Institute of Physics and Natural Sciences Research Institute

University of the Philippines, Diliman

Quezon City, Philippines

E-mail: eestacio@nip.upd.edu.ph

#### **Abstract**

The National Institute of Physics (NIP) was formerly the Department of Physics of the College of Arts and Sciences of the University of the Philippines. In 1983, the Philippine President issued Executive Order 889, establishing the Institute to further strengthen and broaden the national capability to train scientific leaders and conduct research in the basic sciences. The NIP offers both undergraduate and graduate programs in Physics and supports the college's graduate program on Materials Science and Engineering. Moreover, it serves the other colleges and institutes in the university by offering service courses in undergraduate-level physics. The NIP's faculty is composed of 25 Ph.D. (professors and associate professors) and 26 instructors, who are either MS or Ph.D. students, as well. The institute currently hosts five research laboratories working on theoretical physics, instrumentation, photonics, experimental condensed matter physics, computational condensed matter, and is set to expand to newer research areas on gravitation and high energy physics, in the immediate future. As a faculty member belonging to the Condensed Matter Physics Laboratory (CMPL), the particular research area that will be introduced in my talk will be our group's work on terahertz (THz) optoelectronics. The laboratory's interest in terahertz properties of semiconductors started when I returned from my postdoctoral stint from Osaka University and the University of Fukui, where my research dealt mainly on the terahertz characteristics of semiconductors. Having an MBE machine at the NIP, growing III-V semiconductor films and heterostructures, it was logical for me to consider continuing my work on THz optoelectronics and pursue further work on THz antenna devices and other novel THz radiation sources. The talk will conclude with a presentation of the most recent research output of our group on novel THz photoconductive antenna sources as well as on our newest interest on spintronic THz radiation

#### References:

- 1. Afalla, J., et al. A modulation-doped heterostructure-based terahertz photoconductive antenna emitter with recessed metal contacts. Sci. Rep. 10, 19926 (2020).
- 2. Ferrolino, J.P., et al., Thickness dependence of the spintronic terahertz emission from Ni/Pt bilayer grown on MgO via electron beam deposition. Appl. Phys. Express 14, 093001 (2021).
- 3. Prieto, E.A., et al., Trilayer low-temperature-grown GaAs terahertz emitter and detector device with doped buffer. Appl. Phys. Express 13,082012 (2020).
- 4. H. R. et al., Integrated optics spiral photoconductive antennas coupled with 1D and 2D micron-size terahertz-wavelength plasmonic metal arrays. Opt. Mater. Express 12, 1617-1626 (2022).

# Real-time Observation of Surface Chemical Reactions by Wavelength-dispersive Soft X-ray Absorption Spectroscopy



Kenta Amemiya<sup>1,2,3</sup>, Kaoruho Sakata<sup>2</sup>

<sup>1</sup>Graduated School of Pure and Applied Sciences, University of Tsukuba, 1-1-1 Tennodai, Tsukuba, Ibaraki 305-8573, Japan <sup>2</sup>Institute of Materials Structure

Science, High Energy Accelerator Research Organization, 1-1 Oho, Tsukuba, Ibaraki 305-0801, Japan <sup>3</sup>Department of Materials Structure Science, SOKENDAI (The Graduate University for Advanced Studies), 1-1 Oho, Tsukuba, Ibaraki 305-0801, Japan

E-mail: kenta.amemiya@kek.jp

It has long been a challenging task to observe surface chemical reactions without stopping the reaction under near ambient pressure conditions. The X-ray absorption spectroscopy (XAS) is one of the most suitable techniques to quantitatively determine chemical species, but a block of time is needed because the absorption intensity is measured at each energy step by step using a monochromator. We have recently developed a fluorescence-yield wavelength-dispersive XAS technique, by which the XAS data is recorded without scanning the monochromator [1], and the real-time observation of surface chemical reactions under near ambient pressure conditions has been realized [2-4]. The layout of the technique is illustrated in Figure 1. The wavelength-dispersed X rays illuminate the sample, where the wavelength (energy) continuously changes as a function of position, and the fluorescence soft X rays generated at each position on the sample are separately focused by an imaging optics consisting of two spherical mirrors onto each position at the detector. Accordingly, the fluorescence-yield soft X-ray absorption spectrum is obtained without scanning the monochromator. Moreover, the XAS data with different probing depths are simultaneously obtained by collecting the fluorescence X rays at different detection angles, which enables the depth-resolved analysis with sub-nanometer resolution. The time- and depth-resolved observation of the oxidation reactions at Cu and Co surfaces will be presented.

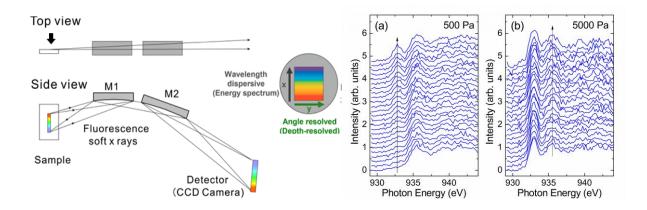


Fig. 1. Experimental setup for the wavelength-dispersive soft X-ray absorption spectroscopy with depth-resolved analysis (left) and soft X-ray absorption spectra taken during the oxidation reaction of a Cu surface under (a) 500 and (b) 5000 Pa oxygen (right).

#### References

[1] K. Amemiya et al., Rev. Sci. Instrum. **2020**, 91, 093104. [2] K. Amemiya et al., e-J. Surf. Sci. Nanotech. **2022**, 20, 135. [3] K. Sakata et al., Nano Lett. **2021**, 21, 7152. [4] K. Sakata and K. Amemiya, J. Phys. Chem. Lett. **2022**. 13, 9573.

### **Student Presentations**

### Development of synthesis method for metalsubstituted-type $\lambda$ -Ti<sub>3</sub>O<sub>5</sub>

Akhmad Fadel Fadilla<sup>1</sup>, Fujisawa Akito<sup>1</sup>, Hiroko Tokoro<sup>1</sup>

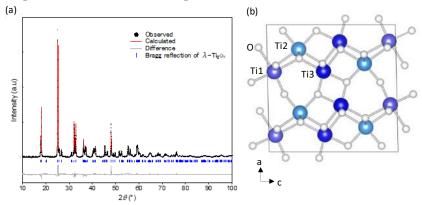
<sup>1</sup>Department of Material Science, Faculty of Pure and Applied Sciences, University of Tsukuba, 1-1-1 Tennodai, Tsukuba, Ibaraki 305-8577, Japan E-mail: s2126033@s.tsukuba.ac.jp



[Introduction] Phase transition materials are a promising and interesting field of study because of their fundamental approach and vast applications e.g., optical memory, heat storage, and sensors. Titanium oxides with various polymorphs offer the phase transition phenomenon between a semiconducting phase and a metallic phase. Among them, it has been reported that the metallic phase lambda type  $Ti_3O_5$  ( $\lambda$ - $Ti_3O_5$ ) nanoparticles show a reversible phase transition with the semiconductor phase beta type ( $\beta$ - $Ti_3O_5$ ) by various external stimuli: light, heat, pressure, and electrical field [1]. This material is expected to be applied as a heat storage material due to its heat storage capability [2]. Controlling material properties is certainly one of the vital aspects of functional technologies and metal doping is one of the most effective approaches. Therefore, it is essential to develop suitable synthesis methods for metal doping. In this study, we developed a new synthesis method of  $\lambda$ - $Ti_3O_5$  nanocrystals that have a possibility of metal substitution.

[Synthesis] Synthesis of  $\lambda$  -Ti<sub>3</sub>O<sub>5</sub> nanocrystals. A microemulsion of H<sub>2</sub>O, TiCl<sub>4</sub>, and NH<sub>3</sub> was prepared in a flask and stirred in an oil bath at 50 °C for 20h to form Ti(OH)<sub>4</sub> precipitate. The precipitate was gained by centrifugation, washed with ethanol, and heated at 60 °C for 24 on a hot plate. The obtained precipitate which was then called by precursor calcinated under hydrogen flow 0.5 dm<sup>3</sup>min<sup>-1</sup> at 1,100 °C for 5h, which produced  $\lambda$  -Ti<sub>3</sub>O<sub>5</sub> nanocrystals.

[Result] Rietveld analysis result of X-ray diffraction (XRD) pattern and crystal structure (Fig.1 (a, b)) shows the obtained sample is a single-phase  $\lambda$ -Ti<sub>3</sub>O<sub>5</sub> (monoclinic system, C2/m; a = 9.8332 Å, b = 3.7857 Å, c = 9.9690 Å,  $\beta = 91.2567$ °). The experiment result shows that the ratio of phase transition from the  $\lambda$ -Ti<sub>3</sub>O<sub>5</sub> to the  $\beta$ -Ti<sub>3</sub>O<sub>5</sub> increases by the applied pressure with the pressure threshold was 300 MPa. In addition, when the pressurized sample is heated, the phase transition from the  $\beta$ -Ti<sub>3</sub>O<sub>5</sub> to the  $\lambda$ -Ti<sub>3</sub>O<sub>5</sub> occurred, and a reversible phase transition due to pressure and heat could be confirmed.



#### References

[1] S. Ohkoshi, Y. Tsunobuchi, T. Matsuda, K. Hashimoto, A. Namai, F. Hakoe, H. Tokoro, *Nature Chem.*, **2**, 539 (2010).

[2] H. Tokoro, M. Yoshikiyo, K. Imoto, A. Namai, T. Nasu, K. Nakagawa, N. Ozaki, F. Hakoe, K. Tanaka, K. Chiba, R. Makiura, K. Prassides, S. Ohkoshi, *Nature Commun.*, **6**, 7037 (2015).

### Abrupt vapor release from porous molecular crystal with visible light

<u>Kentaro Maejima<sup>1</sup></u>, Hiroshi Yamagishi<sup>1</sup>, Ken Albrecht<sup>2</sup>, Youhei Takeda<sup>3</sup>, Yohei Yamamoto<sup>1</sup>

<sup>1</sup>Faculty of Pure and Applied Sciences, University of Tsukuba, 1-1-1 Tennodai, Tsukuba, Ibaraki 305-8573, Japan <sup>2</sup>Institute for Materials Chemistry and Engineering, Kyushu University, 6-1 Kasuga Koen, Kasuga, Fukuoka 816-8580, Japan <sup>3</sup>Graduate School of Engineering, Osaka University, 2-1 Yamadaoka, Suita, Osaka 565-0871, Japan

E-mail: s2220387@s.tsukuba.ac.jp

Water is abundant and useful energy source for inducing chemical or physical reaction. Especially, hydrophilic soft materials can be actuated with moisture, and can reproduce complicated action. However, such operation is difficult to be achieved in reality because of the difficulty of controlling humidity, due to the diffusion of moisture in open space. Thus, simple local humidification device is now necessary for controllable humidity.

Here, we report hydrochromic porous molecular crystal that response to visible light irradiation and release much moisture abruptly. Porous molecular crystal VPC-1 that we discovered previously<sup>[1]</sup> consist of carbazole dendrimer G2DBPHZ (Fig.1a), whose sidechains form myriads of fine pores. VPC-1 absorbs and releases water molecules in its pores spontaneously in response to the humidity around it, and simultaneously changes its color (Fig.1b). And then we found anew that visible light irradiation can also induce the release of moisture from VPC-1, through the measurement of its mass variation. Significant mass decrease was observed with visible light irradiation, and the necessary light intensity for inducing water release is different on the wavelength of irradiated light (Fig.1c). Furthermore, through the temperature measurement during irradiation to VPC-1 powder, it became clear that VPC-1 is heated with irradiation by photothermal effect, and release water molecules.

As attractive application of VPC-1, we tried to create vapor actuator that consist of VPC-1 and cellophane film. Released moisture from VPC-1 with irradiation is absorbed by one side of cellophane film, and the film would bend like bimetal due to the swelling of cellophane (Fig.1d). And VPC-1 can actuate the film larger than activated carbon, a representative porous material, that implies VPC-1 can work as better vapor provider.

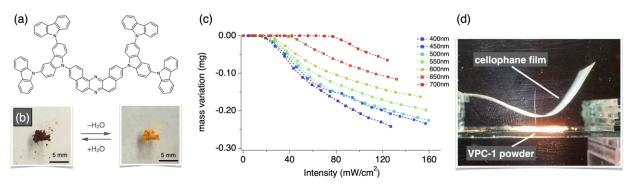


Fig. 1. (a) Molecular structure of G2DBPHZ. (b) Color change of VPC-1 powder upon humidity variation. (c) Wavelength dependency of mass variation upon visible light irradiation. (d) Vapor actuator that consist of VPC-1 powder and cellophane film.

### References

[1] H. Yamagishi et al., Commun. Chem. 2020, 3, 118.

### Study on Mechanism of Fenton Catalyst from Grinding Spark of Waste Metal for Textile Industry Dye Pollutant



Fathan Aditya Sanjaya<sup>1</sup>, Azhar Isti Hanifah<sup>1</sup>, Aysha Rasheeda<sup>1</sup>, Ahmad Affan Farizi<sup>1</sup>, Untung Triadhi<sup>2</sup>, Arie Wibowo<sup>1,3</sup>

<sup>1</sup>Materials Science and Engineering Research Group, Faculty of Mechanical and

Aerospace Engineering, Institut Teknologi Bandung, Jl. Ganesha 10, Bandung 40132 Indonesia <sup>2</sup>Analytical Chemistry Research Group, Faculty of Mathematics and Science, Institut Teknologi Bandung, Jl. Ganesha 10, Bandung 40132 Indonesia, <sup>3</sup>research Center for Nanosciences and Nanotechnology, Institut Teknologi Bandung, Jl. Ganesha 10, Bandung 40132 Indonesia

E-mail: fathansanjaya1@gmail.com

Water is one of the most crucial elements in life, both for humans and for other creatures. One of the resources of water that is widely used in West Java Province is the Citarum river. The Citarum River itself plays a crucial role for the society in West Java. One of the problems that occurs in the Citarum River is waste pollution caused by textile industries activity. Therefore, textile industry wastewater containing residual dyes in the Citarum River watershed has a strong potential to contain azo dye. The release of azo dyes into the environment in the form of liquids from industry is also a major concern in the study of wastewater treatment because azo dyes themselves can be carcinogenic and can cause genetic mutations. Advanced Oxidation Processes (AOPs) themselves have been widely used in the treatment of organic pollutants. Among the variants of AOPs, the Fenton reaction is considered quite attention-grabbing due to its high-performance quality, simple technology and more environmentally friendly. By still referring to the previous research, the use of Fe/Fe<sub>2</sub>O<sub>3</sub> core-shell. The catalyst used was taken from waste material ST37 steel and K100 steel. In this research, the methylene blue takes the role as pollutant model. This research would also focus on the quantification mechanism of degradation carried out by hydroxyl radicals on dye waste using a 2-propanol/nitrobenzene as the probe.

### Modification of Surface Plasmon Resonance (SPR) Biosensor using MoS<sub>2</sub>-MoO<sub>3</sub> Hybrid Microflowers for CFP-10 Tuberculosis Detection

<u>Chandra Wulandari<sup>1,2</sup></u>, Ni Luh Wulan Septiani<sup>2,3</sup>, Gilang Gumilar<sup>2,4</sup>, Ahmad Nuruddin<sup>2</sup>, Nugraha<sup>2,4</sup>, Muhammad Iqbal<sup>2</sup>, and Brian Yuliarto<sup>2,4</sup>

<sup>1</sup>Master Program of Engineering Physics, Faculty of Industrial Technology, Institut

Teknologi Bandung, Ganesha 10, Bandung 40132, Indonesia <sup>2</sup>Advanced Functional Material Research Group, Faculty of Industrial Technology, Institut Teknologi Bandung, Jl. Ganesha No. 10, Bandung, Jawa Barat, 41032, Indonesia <sup>3</sup>Research Center for Advanced Materials, National Research, and Innovation Agency (BRIN), Kawasan Puspiptek, South Tangerang 15134, Indonesia. <sup>4</sup>Research Center for Nanosciences and Nanotechnology (RCNN), Institut Teknologi Bandung, Jl. Ganesha No. 10, Bandung, Jawa Barat, 41032, Indonesia

E-mail: 23320303@mahasiswa.itb.ac.id

Tuberculosis (TB) is a respiratory system disease caused by Mycobacterium tuberculosis (Mtb), with overflow cases and high mortality rates. TB control involves multiple strategies and aspects, including developing rapid detection technology. In this study, we report the surface plasmon resonance (SPR) biosensor with MoS<sub>2</sub>-MoO<sub>3</sub> microflowers modification to detect the secretory protein of TB, CFP-10. The material was suitable for SPR due to high optical absorption, large surface area, and rich edge-active sites<sup>[1]</sup>. The MoS<sub>2</sub>-MoO<sub>3</sub> was prepared by hydrothermal methods with varied pH and trisodium citrate (Na<sub>3</sub>Ct), which were projected to influence the microflowers formation and size<sup>[2,3]</sup>. The materials characterization revealed the best MoS<sub>2</sub>-MoO<sub>3</sub> hybrid microflowers obtained from synthesis at pH 7 with 0.5 g Na<sub>3</sub>Ct (Fig 1(a)). As shown in Fig. 1(b), the modified SPR biosensor response fits the Langmuir-Freundlich adsorption model with positive cooperativity and performs ten times better than the bare Au biosensors. The thicker MoS<sub>2</sub>-MoO<sub>3</sub> resulted in higher detection response, sensitivity, and smaller detection limit (LOD). However, the saturation was found at 15L thickness due to the attenuation of the surface plasmon (illustrated by Fig 1(c)). The Au/MoS<sub>2</sub>-MoO<sub>3</sub> 12L was chosen as the best sensor chip due to excellent sensitivity and LOD of 1.005 and 3.44 ng/mL (S/N = 3), respectively. This biosensor also has good selectivity and reproducibility based on measurement to other analytes and repeated measurements on six different chips. From this study, it has been proven that MoS<sub>2</sub>-MoO<sub>3</sub> hybrid microflowers can significantly improve the performance of SPR biosensors.

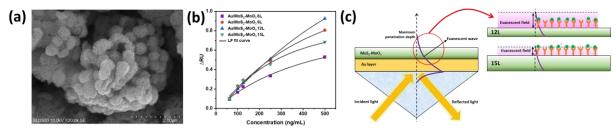


Fig. 1. (a) The SEM images of synthesized MoS<sub>2</sub>-MoO<sub>3</sub> at pH 7 with 0.5 g Na<sub>3</sub>Ct. (b) The CFP-10 concentration vs. ΔRU with LF fit curve for Au/MoS<sub>2</sub>-MoO<sub>3</sub> with different thicknesses. (c) The illustration of evanescent field interaction with targets at 12L and 15L MoS<sub>2</sub>-MoO<sub>3</sub>.

### References

[1] Y. Chen et al., Biosens. Bioelectron. 2022 198 113787. [2] G.H. Jetani et al., Opt. Mater. (Amst). 2022 124 111974. [3] J. Turkevich et al., Discuss. Faraday Soc. 1951 11 55–75.

# Functionalization of Magnetic Fluorescent Silica Nanoparticles with Angiotensin-Converting Enzyme II for Detection of Severe Acute Respiratory Syndrome Coronavirus-2



<u>Muhammad Yovinanda Maulana</u><sup>1</sup>, Ahmad Nurrudin<sup>1,2</sup>, Agustina Sus Andreani<sup>2,3</sup>, Brian Yuliarto<sup>1,2</sup>, Ni Luh Wulan Septiani<sup>2,4</sup>, S. N. Aisyiyah Jenie<sup>2,3</sup>

<sup>1</sup>Advanced Functional Material Research Group, Department of Engineering Physics, Institut Teknologi Bandung, Bandung 40132, Indonesia <sup>2</sup>BRIN and ITB Collaboration Research Centre for Biosensor and Biodevices, Ganesa 10, Bandung 40132, Indonesia <sup>3</sup>Research Centre for Chemistry, National Research and Innovation Agency, Building 452, Kawasan Puspitek, South Tangerang 15314, Indonesia <sup>4</sup>Research Centre for Advanced Materials, National Research and Innovation Agency, Kawasan Puspitek, South Tangerang 15314, Indonesia

E-mail: 23320302@mahasiswa.itb.ac.id

Severe Acute Respiratory Syndrome Coronavirus-2 (SARS CoV-2) first was reported in Wuhan, Hubei Province of China, on December 18, 2019 [1]. In this study, an optical biosensor based on fluorescence nanoparticles was synthesized using natural silica nanoparticles incorporated with fluorescence dye which modified with Fe3O<sub>4</sub> nanoparticles (Fe-NPs) to obtained magnetic fluorescent silica nanoparticles (Fe-FSNP) are made for SARS CoV-2. The receptor used in this biosensor was Angiotensin-Converting Enzyme II (ACE-2). Hydrosilylation process with undecylenic acid then EDC and NHS are used in this activity before functionalized with ACE-2. Samples were characterized by several characterizations instruments to confirm the surface morphology, chemical, physical, and optical properties of the Fe-FSNP samples. Sensitivity performance was observed in the concentration range of SARS-CoV-2 in PBS from 10<sup>-1</sup> to 10<sup>-8</sup> μg/mL. The limit of detection (LOD) was 0.14 fg/mL, calculated using the equation yb + 3Stdb, whereas yb was the mean fluorescence intensity loss measured for the blank control and Stdb was the associated standard deviation [2].

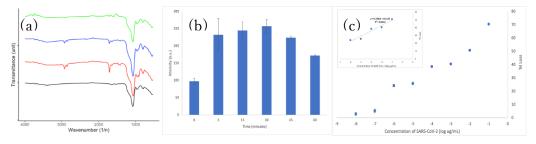


Fig. 1. (a) FTIR spectra of Fe-FSNP (black), Fe-FSNP/COOH (red), Fe-FSNP/EDCNHS (blue), and Fe-FSNP/ACE2 (green). (b) The detection time of SARS-CoV-2 (0,1 mg/mL) by Fe-FSNP/ACE2 in solution The Fe-FSNP/ACE samples were excited at 550 nm with the maximum intensity at 588 nm. (c) The correlation between %Iloss of Fe-FSNP/ACE2 at 588 nm and SARS-CoV-2 concentrations after 30 minutes incubation

### References

[1] S. Iravani, 'Nano- and biosensors for the detection of SARS-CoV-2: challenges and opportunities', *Mater. Adv.*, vol. 1, no. 9, pp. 3092–3103, 2020

[2] F. S. H. Krismastuti, S. Pace, and N. H. Voelcker, 'Porous Silicon Resonant Microcavity Biosensor for Matrix Metalloproteinase Detection', *Adv. Funct. Mater.*, vol. 24, no. 23, pp. 3639–3650, Jun. 2014

### Deep Eutectic Solvent Assisted Ionothermal Synthesis of Cobalt Based Metal-organic Complex as Electrode Material in Supercapacitors

Vidhya Selvanathan<sup>1</sup>, <u>Syaza Amira Razali<sup>1</sup></u>, Jun-ichi Nishida<sup>2</sup>, Masaaki Tomura<sup>3</sup>, Ghulam Muhammad<sup>4</sup>, Huda Abdullah<sup>5</sup>, Akira Watanabe<sup>6</sup>, Md. Akhtaruzzaman<sup>1,7</sup>

<sup>1</sup>Solar Energy Research Institute (SERI), Universiti Kebangsaan Malaysia (UKM), 43600 Bangi, Selangor, Malaysia <sup>2</sup>Graduate School of Engineering, University of Hyogo, 2167 Shosha, Himeji, Hyogo 226-8502, Japan <sup>3</sup>Institute for Molecular Science, Myodaiji, Okazaki 444-8585, Japan 4Department of Computer Engineering, College of Computer and Information Sciences, King Saud University, Riyadh, 11543, Saudi Arabia <sup>5</sup>Department of Electrical, Electronic and Systems Engineering, Faculty of Engineering and Built Environment, Universiti Kebangsaan Malaysia, 43600 Bangi, Selangor, Malaysia <sup>6</sup>Institute of Multidisciplinary Research for Advanced Materials (IMRAM), Tohoku University, Sendai 980-8577, Japan <sup>7</sup>Graduate School of Pure and Applied Sciences, University of Tsukuba, Tsukuba, Ibaraki 305-8573, Japan

E-mail: mirarazali@gmail.com

A combination of cobalt and dipicolinic acid-based metal organic complex was synthesized via deep eutectic solvent (DES) based ionothermal synthesis. The DES comprising of choline chloride and urea served as the solvent medium that cater the formation of novel 3-D layered motif as depicted by the crystallographic data of the complex. FESEM, TEM and EDX analysis verified the formation of unique, hollow morphology and homogeneous distribution of metal ions within the cobalt complex synthesized ionothermally. Based on BET surface area analysis, the presence of micro- and mesopores within the structure was verified. The structurally layered cobalt complex was then used as an electrode material for supercapacitor with a specific capacitance of 712 and 556 F g<sup>-1</sup> at 1.0 and 5.0 A g<sup>-1</sup> respectively. The energy density and power density were calculated to be 5.71 W h k g<sup>-1</sup> and 60.09 W k g<sup>-1</sup> when tested at the current density of 1 A g<sup>-1</sup>. The novel material also showed good cycling stability by retaining at 76% of initial value after over 500 cycles. These values demonstrate that ionothermally synthesized transition metal based organic complexes can serve as prospective electrode material in supercapacitors.

### Developing High Stable Perovskite Solar Cell Using RF Magnetron Sputtered Mo-doped Tungsten Oxide as Electron Transport Layer



Md. Mahfuzul Haque<sup>1</sup>, Samiya Mahjabin<sup>1</sup>, M. S. Bashar<sup>2</sup>, M. S. Jamal<sup>2</sup>, Munira Sultana<sup>2</sup>, Abdur Rahim<sup>2</sup>, Md. Shahiduzzaman<sup>3</sup>, Md. Akhtaruzzaman<sup>1,4,\*</sup>

<sup>1</sup>Solar Energy Research Institute (SERI), Universiti Kebangsaan Malaysia, 43600 Bangi, Malaysia <sup>2</sup>Bangladesh Council of Scientific and Industrial Research, Dhaka 1205, Bangladesh

E-mail: mahfuz.ap@gmail.com

#### Abstract

In this work, RF magnetron sputtering was used to prepare Mo-doped WO<sub>3</sub> thin films under several conditions for proposing the optimum one to use as electron transport layer (ETL) in perovskite solar cell (PSC) [1]. Mo and WO<sub>3</sub> were co-sputtered for different RF power at the Mo target and a fixed power at the WO<sub>3</sub> target. After annealing those thin films, the optimum one has been chosen based on its optoelectronic properties. Then by maintaining the optimum conditions, deposition time was varied to deposit the film of desired thickness. On FTO-coated glass, Mo-doped WO<sub>3</sub> was deposited for optimum RF power and deposition time. After annealing, Cs<sub>0.1</sub>FA<sub>0.9</sub>PbI<sub>3</sub> perovskite layer has been deposited through the spin coating on this ETL. As a hole transport layer (HTL), Spiro-OMeTAD was deposited through spin coating. Finally, as the electrode, Au was deposited by thermal evaporation. This PSC has achieved a power conversion efficiency (PCE) of 8.52%. For testing the stability, the unencapsulated cell was stored in the dark under ambient air without a UV filter at 40-50% relative humidity. After 60 days, PCE dropped by only 18.5% of its initial value, which is surely a great achievement in preparing a PSC with high stability. A promising approach has been established through this study that provides a way of developing a highly stable perovskite solar cell using Mo-doped WO₃ as ETL.

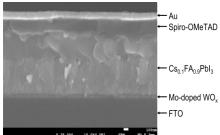


Figure 1. Cross section of fabricated PSC

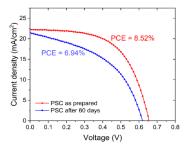


Figure 2. Comparison between J-V curves of the PSCs, as fabricated and after 60 days

### References

1) Md.Akhtaruzzaman, VidhyaSelvanathan "Comprehensive Guide on Organic and Inorganic Solar Cells: Fundamental Concepts to Fabrication Methods" - 1st Edition - November 16, 2021 (Elsevier)

<sup>&</sup>lt;sup>3</sup>Nanomaterials Research Institute (NanoMaRi), Kanazawa University, Kakuma, Kanazawa 920-1192, Japan

<sup>&</sup>lt;sup>4</sup>Graduate School of Pure and Applied Sciences, University of Tsukuba, Tsukuba 305-8573, Ibaraki, Japan

### Molecular Insight into Hybridization of Metal-Organic Frameworks and Choline-based Ionic Liquids (MOF-IL) for Gas Adsorption

Mohd Adil Iman Ishak<sup>1</sup>, Khairulazhar Jumbri<sup>1,2</sup>, Shaari Daud<sup>3</sup>, Mohd Basyaruddin Abdul Rahman<sup>4</sup>, Roswanira Abdul Wahab<sup>5</sup>, Hiroshi Yamagishi<sup>6</sup>, Yohei Yamamoto<sup>6</sup>



<sup>1</sup>Department of Fundamental and Applied Sciences, Universiti Teknologi PETRONAS, 32610, Bandar Seri Iskandar, Perak, Malaysia <sup>2</sup>Centre of Research in Ionic Liquids (CORIL), Universiti Teknologi PETRONAS, 32610 Bandar Seri Iskandar, Perak, Malaysia <sup>3</sup>Faculty of Applied Sciences, Universiti Teknologi MARA, Bandar Jengka, 26400, Bandar Tun Razak, Pahang, Malaysia <sup>4</sup>Department of Chemistry, Faculty of Science, Universiti Putra Malaysia, 43400, UPM Serdang, Selangor, Malaysia <sup>5</sup>Department of Chemistry, Faculty of Science, Universiti Teknologi Malaysia, 81310, UTM Johor Bahru, Johor, Malaysia <sup>6</sup>Division of Materials Science, Faculty of Pure and Applied Sciences, University of Tsukuba, 1-1-1 Tennodai, Tsukuba, Ibaraki, 305-8573, Japan

E-mail: adil iman78@yahoo.com

The compatibility and performance of an Isoreticular Metal-Organic Frameworks (IRMOF-1) impregnated with choline-based ionic liquids (ILs) for selective adsorption of H<sub>2</sub>S/CO<sub>2</sub>, were studied by molecular dynamics (MD) simulation. Cholinium alanate ([Chl][Ala]) was nominated as the suitable IL for impregnation into IRMOF-1, consistent with the low RMSD values (0.546 nm, 0.670 nm, 0.776 nm) at three IL/IRMOF-1 w/w ratios (WIL/ IRMOF-1 = 0.4, 0.8, and 1.2). The [Chl]<sup>+</sup> and [Ala]<sup>-</sup> ion pair was located preferentially around the carboxylate group within the IRMOF-1 framework, with the latter interacting strongly with the host than the [Chl]<sup>+</sup>. Results of radius of gyration (Rg) and root mean square displacement (RMSD) revealed that a ratio of 0.4 w/w of IL/IRMOF-1 (Rg = 1.405 nm; RMSD = 0.546 nm) gave the best conformation to afford an exceptionally stable IL/IRMOF-1 composite. It was discovered that the IL/IRMOF-1 composite was more effective in capturing H<sub>2</sub>S and CO<sub>2</sub> compared to pristine IRMOF-1. The gases adsorbed in higher quantities in the IL/IRMOF-1 composite phase compared to the bulk phase, with a preferential adsorption for H<sub>2</sub>S, as shown by the uppermost values of adsorption (A<sub>H2S</sub> = 17.954 mol L-1 bar-1) and an adsorption selectivity (AS<sub>H2S/CO2</sub> = 43.159) at 35 IL loading.

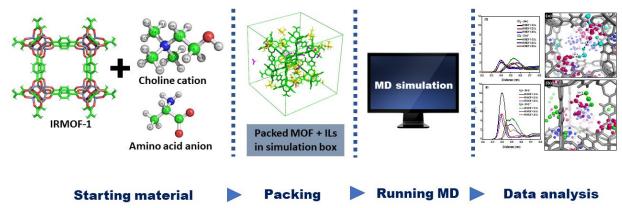


Figure 1: Overall process of MD simulation of IL/IRMOF-1 for H<sub>2</sub>S/CO<sub>2</sub> adsorption.

### Theoretical Studies of Quaternary Ammonium Surfactant Corrosion Inhibitors on Fe (110) in Acetic Acid Media via DFT Calculation and MD Simulation

Mohd Sofi Numin<sup>1</sup>, Khairulazhar Jumbri<sup>1</sup>, Kee Kok Eng<sup>2</sup>

<sup>1</sup>Department of Fundamental and Applied Sciences, Universiti Teknologi PETRONAS, 32610 Seri Iskandar, Perak, Malaysia <sup>2</sup>Department of Mechanical Engineering, Universiti Teknologi PETRONAS, 32610 Seri Iskandar, Perak, Malaysia

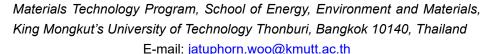


E-mail: sofi.numin@utp.edu.my

Corrosion can cause a major failure to the pipelines and destroy the transportation systems in the oil & gas industry. The addition of corrosion inhibitors (CI) was the most promising method in reducing the corrosion rate of the metal surface in the pipelines. The development of a new CI molecule becomes the primary problem between researchers due to the lack of an in-depth investigation on the CI molecule's mechanism as a corrosion inhibitor. Hence, in this study, density functional theory (DFT) calculation and molecular dynamics (MD) simulation was used to do an in-depth study on the inhibition mechanism of quaternary ammonium surfactant CI molecules with a different chain length in the presence of 1 M HCl and 500 ppm acetic acid on the Fe (110) metal surface. Results from DFT calculation showed that all surfactant CI molecules have good inhibition properties where the ammonium groups (N<sup>+</sup>) act as a reactive center to donate electrons to the metal surface with low band-gap energy (1.26 eV). In the MD simulation, C12 showed the most promising CI molecules with high adsorption energy and binding energy value, low diffusion coefficient towards the corrosion particles and randomly scattered at low concentration that give better adsorption towards the Fe (110) metal surface. The inhibition efficiency of all CI molecules based on computer modelling data and the success of an in-depth study on the theoretical understanding of quaternary ammonium surfactant CI molecules in the acidic medium corrosion system towards metal surface could be used as the future development of new surfactant CI molecules with ammonium-based functional groups.

# Preparation of Au-CsWO<sub>3</sub> Nanocomposites and Near-Infrared Shielding Performance of the Materials: A feasibility study

<u>Chanakarn Piwnuan</u>, Jatuphorn Wootthikanokkhan, Chivarat Muangphat





CsWO<sub>3</sub> has been known as an attractive candidate for use as near infrared (NIR) shielding materials for energy-saving window applications. However, the NIR shielding performance of CsWO<sub>3</sub> in the wavelength ranged between 700 and 1100 nm has yet to be improved. In this work, hybrid materials based on rod-like Au-CsWO<sub>3</sub> were synthesized via seed-mediated growth process. The effects of concentration of Au precursor on crystal structure, morphology, and optical properties of the composite materials were investigated. TEM images revealed the appearance of dumbbell shape Au nanomaterials in the hybrid materials (Fig. 1a). The UV/Vis/NIR spectra of Au-CsWO3 nanocomposites showed the effect of Au precursor on the NIR absorption (Fig. 1b). By increasing the concentration of Au precursor, NIR absorption band shifted to the higher wavelength. Moreover, the nanocomposite with larger amount of Au nanodumbbell contributed to the higher NIR absorption ability. Subsequently, the composite films made from poly(vinyl butyral) (PVB) mixed with different amount of Au-CsWO<sub>3</sub> were prepared, using a micro-compounder and a compression molding process. It was found that percentage IR transmittance through the PVB/Au-CsWO<sub>3</sub> composite film decreased with percentage loading of Au-CsWO<sub>3</sub> (Fig. 1c). Moreover, PVB/Au-CsWO<sub>3</sub> composite film showed lower transmittance in the NIR region, compared to the alternative PVB films loaded with same amount of ATO particles. In this regard, properties of various PVB composite films containing different types and concentration of NIR shielding materials is of our interest and will be presented.

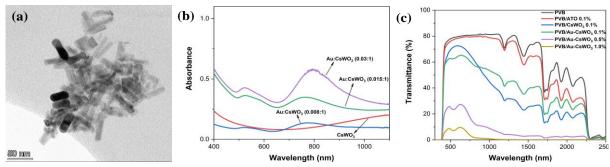


Fig. 1. (a) TEM image of Au-CsWO<sub>3</sub> composite material. (b) UV/Vis absorbance spectra of the nanocomposites with different Au-CsWO<sub>3</sub> mixing ratios. (c) Transmittance spectra of PVB/Au-CsWO<sub>3</sub> composite films with different loading of Au-CsWO<sub>3</sub>.

### Utilization of Cellophane Paper as Flexible Substrates in Perovskite Solar Cells

<u>Wassana Lekkla</u><sup>1,2</sup>, Kanyanee Sanglee<sup>3</sup>, Methawee Nukunudompanich<sup>4</sup>, Surawut Chungchote<sup>1,2,\*</sup>

<sup>1</sup> Department of Tool and Materials Engineering, Faculty of Engineering, King Mongkut's University of Technology Thonburi (KMUTT), 126 Prachauthit Rd., Bangmod, Thungkru, Bangkok 10140, Thailand.



- <sup>2</sup> Research Center of Advanced Materials for Energy and Environmental Technology (MEET), King Mongkut's University of Technology Thonburi (KMUTT), 126 Prachauthit Rd., Bangmod, Thungkru, Bangkok 10140, Thailand.
- <sup>3</sup> Solar Photovoltaic Research Team, National Energy Technology Center, National Science and Technology Development Agency, 111 Thailand Science Park, Phaholyothin Rd., Klong Nueng, Klong Luang, Pathum Thani 12120, Thailand.
- <sup>4</sup> Department of Industrial Engineering, King Mongkut's Institute of Technology Ladkrabang, Chalong Krung 1 Alley, Lat Krabang, Bangkok 10520, Thailand.

E-mail: <u>wassana.lekk@mail.kmutt.ac.th</u> (WL) <u>kanyanee.san@entec.or.th</u> (KS) <u>methawee.nu@kmitl.ac.th</u> (MN) <u>surawut.chu@kmutt.ac.th</u> (SC)

Perovskite solar cells are the most emerging research area among different modern photovoltaic technologies due to the fast development of efficiency. It has improved from 3.5% to 25.8% in a decade. In addition, advantages of perovskite solar cells include superpower conversion efficiency, low-cost, and solution processability. At this time, paper has become an attractive print material for electronics into a wearable due to its flexibility, inexpensive, lightweight, foldable, recyclable and natural disposables. Cellophane paper is also an interesting option because translucent, light, and affordable. In this work, we are interested in fabrication cellophane paper-based planar perovskite solar cells. Indium tin oxide (ITO) was coated on cellophane paper as a transparent electrode with tin oxide (SnO<sub>2</sub>, as an electron transport layer), perovskite (as a light absorber), Spiro-MeOTAD (as the hole transport layer), and silver (Ag, as the electrode). The structural architecture was cellophane/ITO/SnO<sub>2</sub>/perovskite/Spiro-MeOTAD/Ag (Fig. 1). Our discovery contributes an approach to fabricate dependable power source for lightweight electronics in the future.

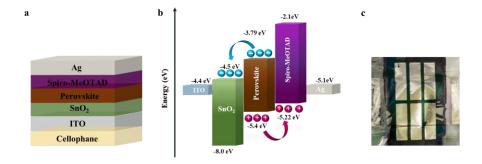


**Fig. 1** (a) Planar layer device architecture of the cellophane-based perovskite solar cell. (b) corresponding energy level diagram. (c) an image of a full device (cellophane/ITO/SnO<sub>2</sub>/perovskite/Spiro-MeOTAD/Ag)

### References

- [1] Roy, Priyanka, et al., 2022. Coatings, 12(8), 1089.
- [2] Gao, Chaomin, et al., 2018. Solar RRL, 2(11), 1800175.

### Recovering of Silicon Wafers for Silicon Fine Particles Production

Saravy Dum, 1,2 Surawut Chuangchote 3,4,\*

<sup>1</sup> The Joint Graduate School of Energy and Environment, King Mongkut's University of Technology Thonburi (KMUTT), 126 Prachauthit Rd., Bangmod, Thungkru, Bangkok 10140, Thailand. <sup>2</sup> Center for Energy Technology and



Environment, Ministry of Education, Bangkok, Thailand. <sup>3</sup> Department of Tool and Materials Engineering, Faculty of Engineering, King Mongkut's University of Technology Thonburi (KMUTT), 126 Prachauthit Rd., Bangmod, Thungkru, Bangkok 10140, Thailand. <sup>4</sup> Research Center of Advanced Materials for Energy and Environmental Technology (MEET), King Mongkut's University of Technology Thonburi (KMUTT), 126 Prachauthit Rd., Bangmod, Thungkru, Bangkok 10140, Thailand. \*Corresponding author. Tel: +66-2-470-9216, Fax: +66-2-872-9080

E-mail: surawut.chu@kmutt.ac.th

Silicon wafer, the semiconductor, is the main component of silicon-based solar cells which carries around sixty percent of the cell cost. Moreover, ready-to-use wafers need the most energyconsumed manufacturing compared to other materials. Therefore, silicon wafers should be reused as many times as possible. Researchers have proposed several etching methods to recover standalone silicon wafers from whole solar cells. Surprisingly, the recovered wafers have identical properties to the original wafers from the industry, which means that they can be reused just like bulk silicon. Here, we demonstrate the chemical etching method to extract silicon and crush them into fine particles for further applications. We divided our work into two sections, (1) the silicon etching and (2) the ball milling (Fig. 1). In the 1<sup>st</sup> section, we used 6M HNO<sub>3</sub> at 160°C for 5 min to remove the cell electrodes, then 85% H<sub>3</sub>PO<sub>4</sub> for 15 min at 70°C to remove the anti-reflection coating and p-n junction, and finally 10M NaOH at 70°C for 5 min to clean all the remaining impurities, followed by ultrasonication in DI water for 10 mins. From that, the bulk wafers were ball-milled using a Fritsch Planetary miller with a 250 ml stainless-still vial and 5 mm balls at 400 rpm for 1 h (with a 10:1 ball-to-powder ratio) under ambient atmosphere and room temperature. The powder was then cleaned using acid treatment to remove the silicon oxide. As a result, fine silicon particles with an average size of not more than 120 nm were obtained with oxygen concentrations of 7.65% and 2.4% before and after acid treatment, respectively.

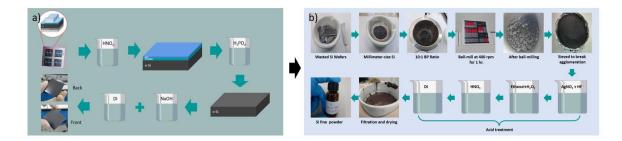
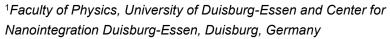


**Fig.1.** Experimental processes: (a) silicon wafer recovering process and (b) fine silicon particle production process.

# Nuclear resonant scattering for hysteresis design of magnetocaloric materials

<u>Johanna Lill</u><sup>1</sup>, Benedikt Eggert<sup>1</sup>, Esen Ercan Alp<sup>2</sup>, Barbara Lavina<sup>2</sup>, Benedikt Beckmann<sup>3</sup>, Michael Hu<sup>2</sup>, Jiyong Zhao<sup>2</sup>, Konstantin Skokov<sup>3</sup>, Katharina Ollefs<sup>1</sup>, Oliver Gutfleisch<sup>3</sup> and Heiko Wende<sup>1</sup>



<sup>&</sup>lt;sup>2</sup> Advanced Photon Source, Argonne National Laboratory, Lemont, Illinois, USA

E-mail: johanna.lill@uni-due.de



Magnetocaloric materials show a significant cooling effect under adiabatic application of alternating external magnetic field [1]. Significant research is performed on this material class, aiming at an environmentally friendly alternative to conventional gas-compression refrigerators as well as for gas liquification applications at cryogenic temperatures [2]. Within the framework of the Collaborative Research Center 270 HoMMage (Hysteresis design of magnetic materials for efficient energy conversion), different approaches to increase the performance of magnetocaloric materials in a cooling cycle are studied. Using nuclear resonant scattering techniques such as nuclear resonant inelastic x-ray scattering (NRIXS) or nuclear forwards scattering (NFS), element-specific contributions of the different subsystems (electronic, magnetic and structural) to magnetostructural phase transition can be resolved, which ultimately determine the performance of the caloric materials [3]. In this talk, nuclear resonant scattering techniques are introduced and applied to magnetocaloric compounds such as the Laves phase DyCo<sub>2</sub>.

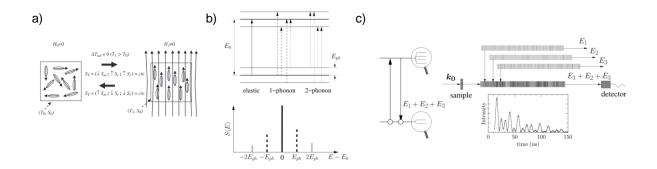


Fig. 1. (a) Systematic representation of the adiabatic cooling cycle using the magnetocaloric effect [4]. (b) Schematic representation of the principal behind nuclear resonant inelastic x-ray scattering (NRIXS), used to determine lattice contributions along the phase transition of magnetocaloric materials [5]. (c) Schematic representation of nuclear forward scattering (NFS), which resolves electronic and magnetic properties of a material [5].

### References

- [1] F. Scheibel et al., Energy Tehnology 2018, 6, 1397-1428.
- [2] T. Gottschall et al., Adv. Energy Mater. 2019, 9, 1901322.
- [3] M. Gruner et al., PRL 114, 057202, 2015.
- [4] J. Romero Gomez et al., Renewable and Sustainable Energy Reviews 2013, 17, 74-82.
- [5] R. Röhlsberger, Nuclear Condensed Matter Physics with Synchrotron Radiation, Hamburg, 2004.

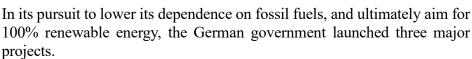
<sup>&</sup>lt;sup>3</sup> Material Science, Technical University Darmstadt, Darmstadt, Germany

# Changing surface morphology and chemistry by scalable atmospheric pressure plasma treatment

Timo Wagner, Nicolas Wöhrl, Axel Lorke

Faculty of Physics and CENIDE, University of Duisburg-Essen, Germany

E-mail: timo.wagner@uni-due.de





The largest of these is the H2Giga project, which focuses its research on scaling up state of the art electrolyzer production and bring next gen electrolyzer technology and materials quickly from the lab to market. H2Giga aims to create optimal conditions for building a 5 GW electrolyzing capacity in Germany by 2030. Within H2Giga we fulfil a special role, as we develop plasma processes for surface modification, which can be used in multiple steps in the production line of the electrodes to optimize production processes and enhance electrode performance. We developed a plasma system that considers industrial compatibility and scalability by design. This includes maximizing treatable surface area, easy adaption to continuous roll-to-roll operation and the ability to operate at up to atmospheric pressures with a large number of possible process gases. A promising application of plasma treatment is the pre-treatment of substrates. For example the surface roughness on a microscopic scale, as well as the surface area can be significantly increased by shortly applying a Nitrogen plasma (Fig. 1). In this talk we present the results of this micro- and nanoscopic structuring and with the Kirkendall effect we discuss a possible underlying mechanism that leads to this kind of structuring in the material.

Another use of plasma treatment in electrode manufacturing is after the coating of the substrates. In electrode manufacturing, a special ink is typically coated onto the nickel, as a catalyst material. One example of a post coating modification is to apply a Nitrogen plasma to the coated electrodes, which leads to a coalescence and/or sintering of the catalyst particles and also yields a porous structure, thus increasing the chemical activity. It is also to be expected to increase the lifetime of the electrodes (Fig. 2).

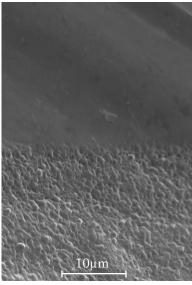


Fig. 1: Roughening by N2

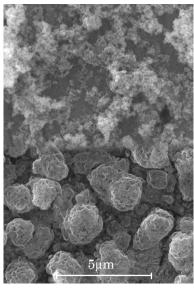
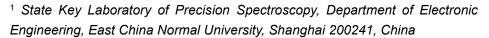
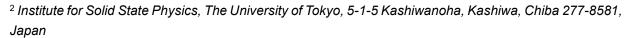


Fig. 2: Catalyst treated with N2

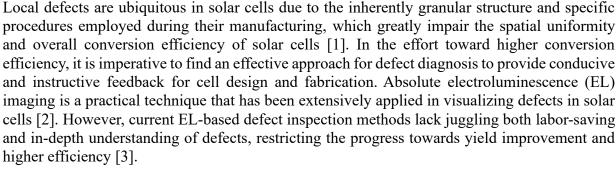
# Computer-Vision-Aided Solar Cell Defect Detection and Classification in Absolute Electroluminescence Imaging

<u>Youyang Wang<sup>1</sup></u>, Jinjia Xu<sup>1</sup>, Xiaobo Hu<sup>1</sup>, Guoen Weng<sup>1</sup>, Shaoqiang Chen<sup>1,2</sup>, Hidefumi Akiyama<sup>2</sup>





E-mail: 52205904001@stu.ecnu.edu.cn



In this work, we propose a computer-vision-aided approach to automatically detect and classify solar cell defects based on absolute EL imaging (Fig. 1a). We first describe the features of solar cell defects by setting several thresholds, then the defect detection is performed according to the described features to locate the defective areas in EL images (Fig. 1b). Based on the detection results, the injection-current-dependent absolute EL intensity loss rates of the detected defects are extracted to perform the defect classification process by matching the numerical simulation results (Fig. 1c). Extensive experiments have been conducted to demonstrate the effectiveness of the approach. The proposed method is expected to provide more guiding feedback in both practical design and reliability diagnosis of the PV industry.

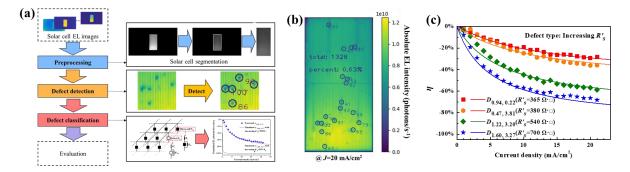


Fig. 1. (a) Overview of the proposed method. (b) Defect detection result of an industry-standard GaAs solar cell, all the tags shown in the EL image are automatically generated by the proposed algorithm. (c) Defect classification results of several detected defects in the GaAs solar cell. The electrical origin of these defects is determined as

#### References

- [1] J. Hong et al., Prog. Photovoltaics Res. Appl. 2020, 28, 295–306. [2] S. Chen et al., Sci. Rep. 2015, 5, 1–6.
- [3] Y. Wang et al., Energy. 2021, 229, 120606.

### Improving Vapor-Transport-Deposited Sb<sub>2</sub>S<sub>3</sub> Thin-

### Film Solar Cells through Source Position

### **Optimization**



<u>Rui Wang<sup>1</sup></u>, Deyang Qin<sup>1</sup>, Yanlin Pan<sup>1</sup>, Guoen Weng<sup>1</sup>, Xiaobo Hu<sup>1\*</sup>, Jiahua Tao<sup>2</sup>, Shaoqiang Chen<sup>1,2,3\*</sup>, Junhao Chu<sup>2</sup>, Hidefumi Akiyama<sup>3</sup>

<sup>1</sup>State Key Laboratory of Precision Spectroscopy, Department of Electronic Engineering, East China Normal University, Shanghai 200241, China <sup>2</sup>Nanophotonics and Advanced Instrument Engineering Research Center, Ministry of Education, East China Normal University, Shanghai 200241, China <sup>3</sup>Institute for Solid State Physics, The University of Tokyo, Kashiwanoha 5-1-5, Kashiwa, Chiba 2778581, Japan E-mail: 52215904004@stu.ecnu.edu

Antimony sulfide (Sb<sub>2</sub>S<sub>3</sub>) is an emerging material with potential applications in photovoltaics, due to its high absorption coefficient, propitious bandgap, non-toxic, and natural abundance of ingredients<sup>[1,2]</sup>. In recent years, The Sb<sub>2</sub>S<sub>3</sub>-based thin-film solar cells have been reported and got some progress in conversion efficiency. Further increased efficiency has been expected through improvements in material quality and device structure.

In this work, we fabricated  $Sb_2S_3$  thin film solar cell by vapor transport deposition and achieved an efficiency improvement from 0.83 to 3.02% by optimizing the position of the evaporation source. The influences on the electrical properties, structural properties, and conversion efficiency of the  $Sb_2S_3$  thin film solar cells were investigated with the J-V measurements, XRD, EQE, and SEM. the results show that the sample at the optimal evaporation source position could obtain the best crystallinity, the strong preferential (221) orientation, and the minimal voids. Meanwhile, the dark J-V curves revealed that the optimal sample had the least Shockley-Read-Hall recombination and the lowest trap concentration. Furthermore, the temperature and light intensity dependent open-circuit voltage measurements demonstrated that the optimal sample exhibits the largest built-in voltage and the lowest carrier recombination rates in all regions including the CdS/Sb<sub>2</sub>S<sub>3</sub> interface, the space-charge region, and the quasi-neutral region thus resulting in the biggest  $V_{oc}$ ,  $J_{sc}$ , and FF, which may contribute to the enhancement of the performance and achieve the highest efficiency.

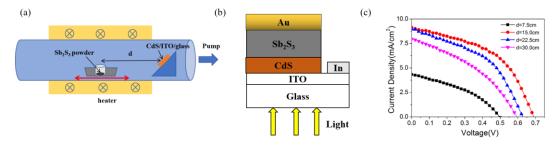
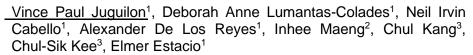


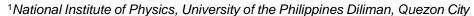
Fig. 1. (a) Schematic diagram of the deposition system for  $Sb_2S_3$  thin films on CdS-coated substrates; (b) Schematic structure of the  $Sb_2S_3$  thin-film solar cell. (c) Light J-V curves of the  $Sb_2S_3$  thin-film cells of d= 7.5 cm, 15 cm, 22.5 cm, 30 cm, respectively.

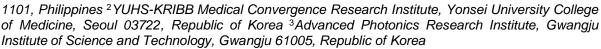
#### References

[1] Y. Yin et al., Sci. Bull 2019, 64, 136–141. [2] S. Yuan et al., Sol. Energy Mater. Sol. Cells. 2016,157, 887–893.

# Carrier capture dynamics in InAs/GaAs self-assembled quantum dots investigated using time-resolved terahertz spectroscopy







E-mail: vjuguilon@nip.upd.edu.ph

We observe the saturation of photoexcited carriers in InAs/GaAs self-assembled quantum dots (QD) at high excitation fluence through an optical pump-terahertz probe (OPTP) experiment conducted at room temperature [1]. Results indicate that increasing the optical pump power leads to a higher photoexcited carrier lifetime immediately upon photoexcitation [2-6]. Calculations show that the lifetime at low pump power (0.4 mW) is 500 ps with a corresponding carrier-to-dot density of 3.69. Meanwhile, at 7.0 mW pump power, a carrier lifetime of 3.7 ns was determined with a 64.62 carrier-to-dot density. For all optical pump powers considered, carrier lifetime decreased to about 500 ps after sufficient time. Previous studies have reported a decrease in the lifetime of the GaAs substrate by an order of magnitude due to the ultrafast carrier capture into the InAs QDs. However, at higher excitation fluence, filling of QD states can occur and this decrease in the effective lifetime is mitigated [2,7]. After recombination of carriers in the dot, QDs will return to its unsaturated state and carrier capture process from the GaAs barrier to the InAs QDs will proceed. These changes in the dynamical processes are reflected in the gradual decrease and convergence of lifetime back to 500 ps.

### References

[1] M.C. Beard, G.M. Turner, and C.A. Schmuttenmaer, *Phys. Rev. B Condens. Matter* **62**, 2000, 15764. [2] D. Turchinovich, K. Pierz, and P. Uhd Jepsen, *Phys. Status Solidi C* **0**(5), 2003, 1556. [3] H.P. Porte, P. Uhd Jepsen, N. Daghestani, E.U. Rafailov, D. Turchinovich, *Appl. Phys. Lett.* **94**(26), 2009, 262104. [4] D.A. Yarotski, R.D. Averitt, N. Negre, S.A. Crooker, A.J. Taylor, G.P. Donati, A. Stintz, L.F. Lester, and K.J. Malloy, *J. Opt. Soc. Am. B* **19**(6), 2002, pp. 1480-1484. [5] Q. Li, Z.Y. Xu, and W.K. Ge, *Solid State Commun.* **115**, 2000, pp. 57-108. [6] T. Muller, F.F. Schrey, G. Strasser, and K. Unterrainer, *Appl. Phys. Lett.* **83**, 2003, 3572. [7] P.A. Loukakos, C. Kalpouzos, I.E. Perakis, Z. Hatzopoulos, M. Sfendourakis, G. Kostantinidis, and C. Fotakis, *J. Appl. Phys.* **91**, 2002, p. 9863.

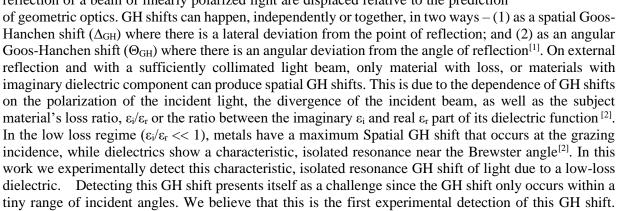
## Goos-Hänchen Shifts in low-loss dielectrics: Experimental observations in Si substrate

### Jared C. Operana<sup>1</sup>, Nathaniel Hermosa<sup>1</sup>

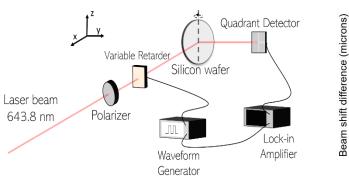
<sup>1</sup>National Institute of Physics, University of the Philippines Diliman, C.P. Garcia Avenue, Diliman, 1127 Quezon City, Philippines

E-mail: joperana@nip.upd.edu.ph

The Goos-Hanchen (GH) shift is a phenomenon where the point and angle of reflection of a beam of linearly polarized light are displaced relative to the prediction



Our setup is shown in Fig. 1a, where the light beam is prepared such that, it is collimated and with a defined polarization. A variable retarder controlled by a waveform generator toggles the polarization between the s- and p-states, before it is made to impinge the Si wafer, our low loss material. The deflection between the two polarization states is measured by the quadrant detector where the deflection of the s-polarized beam is set as the reference. A lock-in amplifier is used to remove technical noise. We detect the  $\Delta$ GH in the range of incident angles between 75.5° and 76°, with the peak recorded at 75.7° (Fig. 1b). We measure a maximum GH shift of  $5.1 \times 10^{-5}$  meters. Lower than 75°, we fail to detect  $\Delta$ <sub>GH</sub> within our limit of precision. We believe that it can be used for applications such as in precision detection [3] and in material characterization. [4]



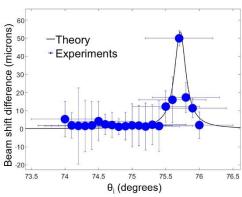


Fig. 1. (a) Experimental setup of GH shift detection, comprising of a light source, a polarizer, variable retarder controlled by a waveform generator in sync with the lock in amplifier and the quadrant detector. Silicon wafer is rotated around its z axis to cover the range of incident angles. (b) Measured beam shift difference, or the difference between GH shifts measured at s and p states of the reflected light.

- [1] Merano, M., Aiello, A., Van Exter, M. P., Eliel, E. R., & Woerdman, J. P. (2007). Observation of Goos-Hänchen shifts in metallic reflection. Optics express, 15(24), 15928-15934.
- [2] Götte, J. B., Aiello, A., & Woerdman, J. P. (2008). Loss-induced transition of the Goos-Hänchen effect for metals and dielectrics. Optics express, 16(6), 3961-3969.
- [3] Olaya, C. M., Hayazawa, N., Hermosa, N., & Tanaka, T. (2020). Angular Goos–Hänchen Shift Sensor Using a Gold Film Enhanced by Surface Plasmon Resonance. *The Journal of Physical Chemistry A*, 125(1), 451-458.
- [4] Zambale, N. A. F., Sagisi, J. L. B., & Hermosa, N. P. (2019). Goos-Hänchen shifts due to graphene when intraband conductivity dominates. Optics Communications, 433, 25-29.











Universiti Kebangsaan Malaysia The National University of Malaysia









